Biogeochemical interactions between aged cementitious materials and sulfate reducing microbial community with propionate as electron donor in the context of nuclear waste repository

Nadège Durban, Alexandra Bertron, Vanessa Sonois-Mazars, Maud Schiettekatte, Gerald Matar, Pierre Albina, Achim Albrecht, Jean-Charles Robinet, Benjamin Erable

Biogeochemical interactions between aged cementitious materials and sulfate reducing microbial community with propionate as electron donor in the context of nuclear waste repository

Nadège Durban [1,2], Alexandra Bertron [1*], Vanessa Sonois-Mazars [1], Maud Schiettekatte [1], Gerald Matar [1,2] ; Pierre Albina[1,2], Achim Albrecht [3], Jean-Charles Robinet [3], Benjamin Erable [2]

[1] Laboratoire Matériaux et Durabilité des Constructions, Université de Toulouse, UPS, INSA. 135 avenue de Rangueil, 31077 Toulouse CEDEX 04, France; nadege.durban@gmail.com (N.D.); bertron@insa-toulouse.fr (A.B.); vmazars@insa-toulouse.fr (V.M.); schiette@insa-toulouse.fr (M.S) ; matar@insa-toulouse.fr (G.M.); pierre.albina@outlook.fr (P.A.)

[2] Laboratoire de Génie Chimique, Université de Toulouse, CNRS, INPT, UPS, 31030 Toulouse, France; benjamin.erable@ensiacet.fr (B.E.)

[3] Andra (Agence nationale pour la gestion des déchets radioactifs), 92298 Châtenay-Malabry, France; achim.albrecht@andra.fr (A.A.); jean-charles.robinet@andra.fr (J. C.R.)

* Corresponding author: postal address: LMDC, INSA Toulouse, 135 avenue de Rangueil, 31077 Toulouse, Cedex 4, France. Email: bertron@insa-toulouse.fr

Abstract

Heterotrophic microbial sulfate reduction can occur in both natural and engineered systems. The process can influence the radionuclide speciation and mobility in deep repository of radioactive waste (DRRW). DRRW are characterised by significant masses of concrete, imposing alkaline pH in the waste cell. This paper aims to evaluate microbial sulfate reduction coupled with propionate oxidation influenced by the alkalinity of the environment: moderate alkaline pH close to 9.0 without cement paste, and moderate alkaline pH which was then moderately increased (pH 9.0 to 9.4) by the

presence of pre-aged solid cement pastes via advanced and moderate ageing protocols, respectively. Regardless of the degree of ageing of the cement pastes, the sulfate reduction rate decreased by up to 84% when the pH increased from 9.0 to 9.4 in the presence of cement paste and by up to 90% in the absence of cement paste. No sulfate reduction or propionate oxidation was observed for pH > 9.5. Microbial metabolites, sulfide, CO_2 and acetate, produced from the reduction of sulfate and oxidation of propionate, and the presence of the microorganisms attached to the cement pastes (composed of up to 80% of sulfate reducing bacteria) led to their biodeterioration. Sulfide enrichment, precipitation of secondary ettringite, and intensified decalcification were notably detected. Self-healing like phenomena were also observed: calcium leached from the cementitious phases reacted with carbonate produced by microorganisms to form of calcium carbonate relocated either in the micro-cracks or on the surface of the pre-aged solid cement pastes.

Keywords: Sulfate-reducing bacteria; cementitious materials; nuclear waste repository; biodeterioration, moderately alkaline pH

1. Introduction

The management of toxic and radioactive waste often relies on clay rocks as a geological barrier and concrete as an engineered barrier to isolate the wastes from the biosphere. Many types of these wastes contain organic matter in various forms (Abrahamsen et al., 2015), some of which are known to complex both toxic metals and radionuclides present in the waste, thus increasing their solubility and mobility (Davis, 1984). For the case of radioactive waste, classified as high-level, intermediate-level or low-level radioactive waste based on its radionuclide content and activity (Ewing et al., 2016), the role of clay, as host rock, and concrete, as major engineering material, needs to be considered explicitly in the assessment of biogeochemical reactions. In France, an ongoing industrial project aiming at constructing a radioactive waste repository within Callovo-Oxfordian (COx) host rocks at a depth of 500 metres is planned for storing high-level waste and long-lived intermediate-

level radioactive wastes (LLILW) in concrete matrices (Albrecht et al., 2013; Rafrafi et al., 2017, 2015). The stabilized LLILW will be cast in cylindrical concrete and / or steel containers, which constitute the primary packages, and will be grouped into secondary packages made of reinforced concrete (Rafrafi et al., 2017, 2015). After closing of the waste galleries, the infiltration of ground water within the storage cells is intended and is expected to induce leaching processes at the interface of cementitious and waste materials, notably. Due to these leaching phenomena, progressive enrichment of the infiltrated water is expected, such as an enrichment in cations (Ca^{2+}, Na^{+}, K^{+}) and hydroxide anion, which impose an alkaline pH, due to the leaching of concrete material (Bertron, 2014). An enrichment in dissolved organic matter or oxyanions released by the radioactive waste (Abrahamsen et al., 2015) is also expected. The leaching of some of these dissolved organic acids may promote the mobility of some usually immobile radionuclides by complexing them, thus affecting the safety of the repository over time, by increasing the risk of contamination of the host rock (Abrahamsen et al., 2015; Albrecht et al., 2013). Biological activity has been observed in the context of in-situ experiments in the Meuse/Haute Marne underground research laboratory in the presence of organic matter (Vinsot et al., 2008a). Therefore, a biotic oxidation of soluble organic acids can be expected in the future within the storage. Organic acids would thus be less available to form complexes with radionuclides and would therefore limit their migration into the host rock and thus improve the safety of the system. The oxidation of organic matter by microorganisms under anaerobic conditions can take place without an electron acceptor, as a fermentation process, or in the presence of an electron acceptor such as nitrate (denitrification process) or sulfate (sulfate reduction process) (Muyzer and Stams, 2008). Sulfate is an oxyanion of wider importance as an electron acceptor, given its high solubility. It may be introduced by natural water during resaturation (Vinsot et al., 2008b) and released from the waste package (bituminized waste or in resin) or cement material (Abrahamsen et al., 2015; Dauzères et al., 2014; van Loon and Hummel, 1999). With a very low standard reduction potential, i.e. $E^{0'}$ for sulfate/sulfite redox couple: -516 mV, the sulfate reduction is not thermodynamically favourable but it could be catalysed by sulfate-reducing bacteria

(SRB) under anaerobic conditions with a temperature below 60°C (Machel, 2001). SRB are versatile in terms of their metabolism and their capacities to use different sources of organic or inorganic matter (Muyzer and Stams, 2008) and the environmental conditions under which they can thrive: anaerobic wastewater treatment plants, marine and fresh water sediments, hydrocarbon seeps, hypersaline environments such as marine sediment, acid mine drainage contaminated sites, or soda lakes, where pH can be higher than 10 (Muyzer and Stams, 2008; Pallud and Van Cappellen, 2006; Sorokin et al., 2014). The metabolism of SRB is increasingly being studied for industrial applications, such as the bioproduction of metal metallic sulfide nanoparticles (such as zinc sulfide) and bioplastic (polyhydroxyalkanoate), and also for industrial wastewater treatment (Duran and Seabra, 2012; Hai et al., 2004; Qian et al., 2019; Ragu Nandhakumar et al., 2022). Very few studies have investigated the reduction of sulfate rate (SRR) at alkaline pH. Some studies have reported SRRs of the order of 18 mM/d at pH 9.0 in haloalkaliphilic media (Sousa et al., 2015) or 0.023 mM/d at pH 9.5 (Mu et al., 2019). Their sensitivity to environmental physicochemical parameters, such as pH, salinity, source of organic matter and temperature, are particularly mentioned in the literature (Gutierrez et al., 2009; Muyzer and Stams, 2008; Qian et al., 2019; Sorokin et al., 2014; vanGinkel et al., 1997). However, the reduction of sulfate by SRB in a cementitious environment, and more precisely under conditions close to those found in nuclear waste repositories, has not been studied. However, it is important to evaluate the sulfate reduction as well as the oxidation rate of organic matter (i.e. propionate here) and the impact of pH on these reactions in order to reduce uncertainties in predictive models of the geochemical evolution of storage cells in underground nuclear waste repositories.

As mentioned earlier, in the absence of an electron acceptor, organic matter can be oxidized in the presence of micro-organisms by fermentation. Alkaline fermentation (i.e. at pH 10) produces very little methane (methanogenic process inhibited) but in comparison to neutral or slightly acidic pH values, this fermentation induces production of up to three times more VFAs (Chen et al., 2021), acetate and propionate being the main VFAs produced (Liu et al., 2014). Propionate has also been found as a degradation product of complex organic matter (such as isosaccharinic acid) identified in

LLIL nuclear waste (Abrahamsen et al., 2015; Kuippers et al., 2015; Rout et al., 2015). For this reason, propionate was chosen as the model organic material in this study, in order to investigate the oxidation of organic matters coupled with the sulfate reduction.

In this context, the objectives of the work presented in this manuscript were (i) to identify the pH limits up to which biological oxidation of propionate can be achieved via reduction of sulfate, and (ii) to measure the propionate oxidation and sulfate reduction rates in an environment like the one of the French nuclear waste repository project (moderate alkaline pH imposed by cementitious material leaching, and anaerobic conditions), and (iii) to study the possible interaction between microorganisms and cementitious materials from two perspectives. First, we observed the colonization of the material surfaces by microorganisms. And secondly, we observed the impact on the materials of the vicinity of biological activity producing sulfides, organic acids and other aggressive compounds that can promote the alteration of cementitious material (Bertron, 2014; Voegel et al., 2019b).

In order to assess the effect of moderately alkaline environment, the experiments were conducted at pH between 8.5 and 10. Moreover, to mimic short-term and long-term cement ageing in the nuclear waste repository (Bertron, 2014; Lagerblad and Traegaardh, 1994; Sellier et al., 2011), the cement pastes used underwent two different levels of alteration (a moderate aging (MA) and an advanced aging (AA)) where three different ratios of solid surface area to liquid volume were applied. In order to investigate biogeochemical interactions between cementitious matrices and microorganisms, the SRRs and the propionate oxidation rates (PORs) were calculated for different ratios of surface area (SA) to liquid volume (V), i.e. SA/V, and for different pH values. Indeed, increasing the SA/V ratio lead to an increase in the alkalinity of the reaction medium in terms of pH and cation concentration from the cementitious matrices leaching. Microscopic observations and complementary experiments were also performed in order to investigate the presence of microorganisms adhering to the cement paste surfaces. To evaluate the level of alteration induced by biological activity on cement paste surfaces,

127 microstructure analyses were performed and the chemical composition of the cement pastes was
128 determined before and after their exposure to the microbial redox activity.

129 ## 2. Materials and methods

130 ### 2.1. Preparation of cementitious material

131 Cement pastes were prepared according to the French standard NF EN 196-3A1. Samples of
132 CEM V/A (S-V) 42.5 N CE PM-ES-CP1 NF, from the Calcia cement factory of *Rombas* (France) were
133 prepared with a water-to-cement ratio of 0.4 (Durban et al., 2020, 2018; Rafrafi et al., 2017) and
134 were cast in hermetic cylindrical moulds 50 mm high and 50 mm in diameter. The cement pastes
135 were maintained at high relative humidity (> 98 %) and 22°C for hardening during 28 days. They were
136 then sawn into 5- or 9-mm thick slices, and each slice was sawn into eight parts to obtain coupons
137 with a projected surface area of respectively 8 or 11 cm^2. The surfaces of the final cement coupons
138 were polished using silicon carbide polishing disks (P120 - ≈ 127 µm - Presi®) to obtain a
139 homogeneous surface roughness (Durban et al., 2020; Voegel et al., 2019b, 2019a).

140 To prepare cement leachate solutions, 2 g of crushed cement paste (granulometry 0.5 - 1.25
141 mm) was stirred (800 rpm) into 2L of ultra-pure water deaerated with nitrogen gas in order to limit
142 carbonation phenomena between leached calcium and CO_2 solubilized in the water. The leaching
143 process maintained anaerobically was stopped when the water solution conductivity reached
144 between 500 and 550 µS/cm with a pH above 11.0. Finally, the cement leachate was filtered and
145 then stored at 4°C in hermetically sealed bottles saturated by nitrogen gas or used immediately
146 (Albina et al., 2021). The chemical composition of the cement leachate solution was analysed using
147 Inductively Coupled Plasma-Optical Emission Spectrometry (ICP-OES) and the results are reported in
148 Table S.1.

149 ### 2.2. Ageing processes for cement pastes

150 A typical cement leachate from freshly poured cement paste has an alkaline pH between 12 and 13.
151 This high pH value decreases with time due to various ageing processes that enhance leaching of
152 hydroxide ions and cations such as calcium ions (Bary, 2008; Bertron, 2014; Gallé et al., 2006; Planel

et al., 2006). Two ageing protocols were set up in order to mimic short-term and long-term cement ageing in the nuclear waste repository.

2.2.1 Advanced ageing process

Cement paste coupons with a thickness of 9 mm (projected surface area 11 cm^2) were firstly immersed in bottles containing 1 L of 0.28 mM acetic acid solution supplemented with 1 mM NaOH to reach pH 4 for three days (solid surface area to liquid volume ratio 64 cm^2/L). The solution was renewed as soon as the pH was higher than 4.3 (Bertron et al., 2007; Larreur-Cayol et al., 2011). Secondly, the coupons were immersed in ultra-pure water for seven days with 3 renewals of the solution in order to remove all traces of acetic acid. During the ageing process, the bottles were continuously stirred (800 rpm), at room temperature, and N_2 bubbling was applied after each solution renewal in order to avoid carbonation phenomena. Alteration of cementitious materials by acetic acid has been thoroughly investigated, and this technique allows fast leaching of hydroxide (OH^-) and alkaline cations (Ca^{2+},Na^+, K^+) without promoting any secondary precipitation or any specific interactions between the acetate anion (CH_3COO^-) and the cations leached from cement pastes (Bertron et al., 2007, 2005a, 2005b; Bertron and Duchesne, 2013). The cement samples treated in this way were labelled AA (advanced ageing).

2.2.2 Moderate ageing process

Cement paste coupons were immersed in 2 L (solid surface area to liquid volume ratio 43 cm^2/L) of ultra-pure water at room temperature for 8 days, under agitation (800 rpm) and N_2 bubbling, the water being renewed on a daily basis. Compared to the advanced ageing process, the moderate ageing process creates less damage to the surface of cement pastes (Duchesne and Bertron, 2013). The stock of cementitious cations (alkalis) (Ca^{2+}, Al^{3+}, Na^+, K^+) and hydroxide (OH^-) ion in the moderately aged cement coupons, and in particular in the surface layer, was thus higher than that in the AA cement paste coupons. The moderately aged cement pastes were labelled MA (moderate ageing).

2.3. Inoculum for the bioreactors

The biological inoculum was a microbial consortium collected from activated sludge of the wastewater treatment plant in Castanet, France. In order to concentrate the inoculum and remove soluble organic substrates from the sludge, 250 mL of the collected mixed liquor was centrifuged at 4600 g at 6°C for 15 min. Finally, the bioreactors were inoculated with 2.8 g/L of dewatered sludge.

2.4. Experiments in bioreactors

250 mL sterile glass bottles having a rubber septum and a screw cap with an aperture were used as anaerobic bioreactors. The bioreactors were protected from light and operated in fed-batch, in anaerobic conditions and at 30 °C. Biological propionate oxidation coupled with sulfate reduction was investigated first in the cement leachate and then in the presence of AA or MA cement paste coupons. The experiments were organized in three successive steps: [step 1] a period of acclimatization for the biological inoculum, with a progressive pH increase from 8.0 to 9.0 in the cement leachate without cementitious material; [step 2] evaluation of the propionate oxidation rate (POR) and the sulfate reduction rate (SRR) without cementitious material; and [step 3] introduction of cement paste coupons, after 20 days for AA and 26 days for MA cement pastes coupons. Before starting each step, the liquid phase of the bioreactor was deaerated by N_2 gas bubbling for 15 min. During all the steps, regular supplementation with 5.7 mM of neutralized propionate and 10 mM of disodium sulfate was performed (Figure 1). At the end of the experiment, to confirm the presence of bacteria attached to the cement paste surface and to characterised the reactivity of microorganism attached, the protocol described by Durban et al. (2020) was adapted and applied (see section S.1 in supplementary material). The bacterial community was also investigated according to the protocol described by Durban et al. (2020) (Section S.2 in supplementary material).

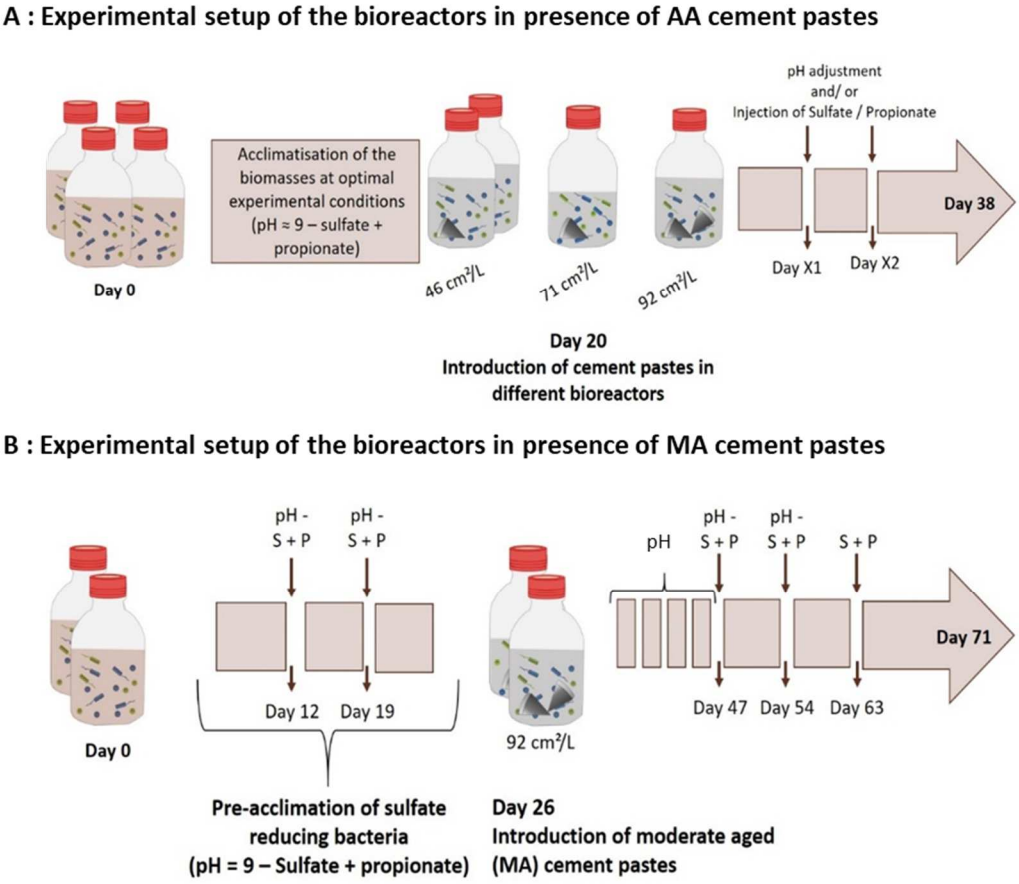

Figure 1: Experimental set-up of the bioreactors to study propionate oxidation and sulfate reduction in presence of A) advanced aged (AA) cement paste coupons and B) moderate aged (MA) cement paste coupons. The pH was adjusted throughout the experiment, while propionate and sulfate were added depending on the reactors as represented: pH: pH adjustment, S: Sulfate supplementation, P: Propionate supplementation.

2.4.1 Experiments in the presence of AA cement paste coupons

A first set of experiments was carried out using four bioreactors containing inoculated cement leachate supplemented with 5.7 mM of propionate neutralized with NaOH (pH: 7.5) and 10 mM of disodium sulfate. The pH was initially adjusted to 8 and was progressively increased with NaOH 1M addition to reach 9, i.e. a moderately alkaline condition. During [step 2], after sulfate and propionate supplementation, the liquid phases in the bioreactors (see section 2.5) were sampled to evaluate the POR and the SRR. For [step 3], AA cement paste coupons were added at increasing surface to volume ratios (area of cement paste surface/cement leachate volume: 46, 71 and 92 cm^2/L), in order to increase the effect of the cementitious material on microbial activity (Figure 1.A). The pH was maintained at values between 9 and 9.5 using hydrochloric acid (1M).

2.4.2 Experiments in the presence of MA cement pastes

A second series of experiments was carried out using two bioreactors supplemented with 5.7 mM of propionate neutralized with NaOH (pH: 7.5) and 10 mM of disodium sulfate. The initial pH was adjusted to 8.8 and the PORs and SRRs were evaluated [step 2]. For [step 3], the MA cement paste coupons were added at day 26 (Figure 1.B) with a surface to volume ratio of 92 cm^2/L. The pH was maintained between 10 and 9.0 for 16 days by using hydrochloric acid (1M). Once the pH was stabilized, the liquid phase in bioreactors (see section 2.5) was regularly sampled to evaluate the PORs and the SRRs in the presence of cement paste.

2.5. Chemical analysis of the inoculated cement leachate

For the samples collected with sterile syringes from the liquid fraction of the bioreactors, i.e. the inoculated cement leachate, the pH was immediately measured using a Eutech Instruments 6500 pH/ ion meter, and to monitor microbial growth, the optical density was measured at 600 nm using a JENWAY 7315 spectrophotometer (Rafrafi et al., 2015).

2 mL of collected solutions were also filtered using 0.2 µm filters (196 Minisart® PES, Sartorius) for analyses of ionic species. The concentrations of propionate, acetate, sulfate, sulfite and thiosulfate were quantified by High Performance Ion Chromatography (Dionex ICS-2000 and ICS-3000) according the protocol described by Alquier et al. (2014) modified according the KOH gradient described in Table S.2.

2.6. Analyses of solid cementitious materials

2.6.1 Microstructural observation and chemical analyses with scanning electron microscopy (SEM) coupled to energy dispersive X-ray spectroscopy (EDS)

The microstructural and chemical characteristics of the aged cement coupons before and after their exposure in the bioreactor were analysed by SEM- EDS (JEOL 6380-LV coupled with XFlash 6/30 Bruker EDS detector). The cement paste coupons were sawn perpendicularly to their flat surfaces. One portion of the specimen was embedded in epoxy resin (Mecaprex Ma2+, Presi). The sawn surface comprising the outer zone and the unaltered core of the specimen was dry polished with silicon carbide polishing disks (Presi) (polishing disc references and grain sizes: ESCIL, P800–22 µm,

P1200–15 µm and P4000–5 µm). The polished sections were then coated with carbon (Giroudon et al., 2021; Voegel et al., 2019a).

2.6.2 Mineralogical analyses with X-ray diffraction (XRD)

The mineralogical composition of the cement paste coupons was analysed before and after their exposure in the different bioreactors using X-ray diffraction (BRUKER D8 Advance, Cu cathode, 40 kV, 40 mA). An initial analysis was carried out on the external surface of the coupons that was directly exposed to the liquid fraction of the bioreactors. Then the external layer was cautiously scraped using silicon carbide polishing disks (P120 - ≈ 127 µm - Presi®), until a depth of 100-200 µm was achieved. This procedure was repeated several times to remove the precipitates from the surfaces of cement pastes, if any, and to eliminate the altered zones until unaffected core was reached within the cement coupons (Bertron et al., 2009).

2.7. Fluorescence microscopy

Biofilms attached and developed on the cement paste coupons were chemically fixed following a specific biofilm fixation protocol on cement pastes, as described previously (Durban et al., 2020; Voegel et al., 2015). The labelling step consisted of submerging the coupons in a mixture of PBS (phosphate buffered saline) solution and SYTO® 9 (Invitrogen, USA) for 10 minutes. The final step before microscopic visualization consisted of rinsing the cement coupons with 10 mM PBS solution (phosphate buffered saline - Commercial tablets pH 7.2, Applichem), to remove excess dye (Durban et al., 2020). Sample visualization was performed using a Carl Zeiss Axiomalger M2 microscope designed for epifluorescence detection and equipped with an HBO 200 W/4 and Zeiss set 09 as a filter (excitor HP450-490, reflector FT 10, barrier filter LP520). Images were acquired using a monochrome digital camera, and several acquisitions (about 70 images) were performed and compiled using the Zen blue software. To avoid potential rapid carbonation of the cement coupon during the imaging, the cement coupons were immersed in a 10X PBS solution.

3. Results

Reactors under abiotic conditions were operated to evaluate the reactivity of the systems in the absence of microorganisms. No uptake was observed for propionate, a low uptake of sulfate (0.02 -

0.04 mM/d) was observed (result are availed as supplementary data Figure S.3). A white needle-like deposit (ettringite) was observed on the surface of the cement pastes in SEM (data not shown).

3.1 Assessment of the microbial propionate oxidation and sulfate reduction in the presence of AA cement paste coupons

3.1.1 Analysis of the liquid fraction of the bioreactors

The SRR and POR were investigated in the presence and absence of AA cement paste coupons with different solid surface area to liquid volume ratios (SA/V ratios): the two duplicates for 46 cm^2/L, and 71 and 92 cm^2/L. The results were very similar for the four bioreactors. Consequently, only the results of the bioreactor containing the SA/V ratio of 71 cm^2/L is discussed below and the results of the other ratios studied are reported in the supplementary data (Figure S.4, Figure S.5 and Figure S.6). Figure 2 thus shows the evolution of the pH (Figure 2.a) and the optical density (OD) at 600 nm (Figure 2.b) in the bioreactor containing the SA/V ratio of 71 cm^2/L, and the evolution of concentrations of sulfate, sulfite, and thiosulfate (Figure 2.c), and propionate and acetate (Figure 2.d), between day 17 and the end of the experiment. AA cement paste coupons were incorporated into the bioreactor at day 20. The data collected between day 0 and day 17 cover the period of acclimation to the pH increase from 8 to 9 (step 1) and are not of interest for the current study.

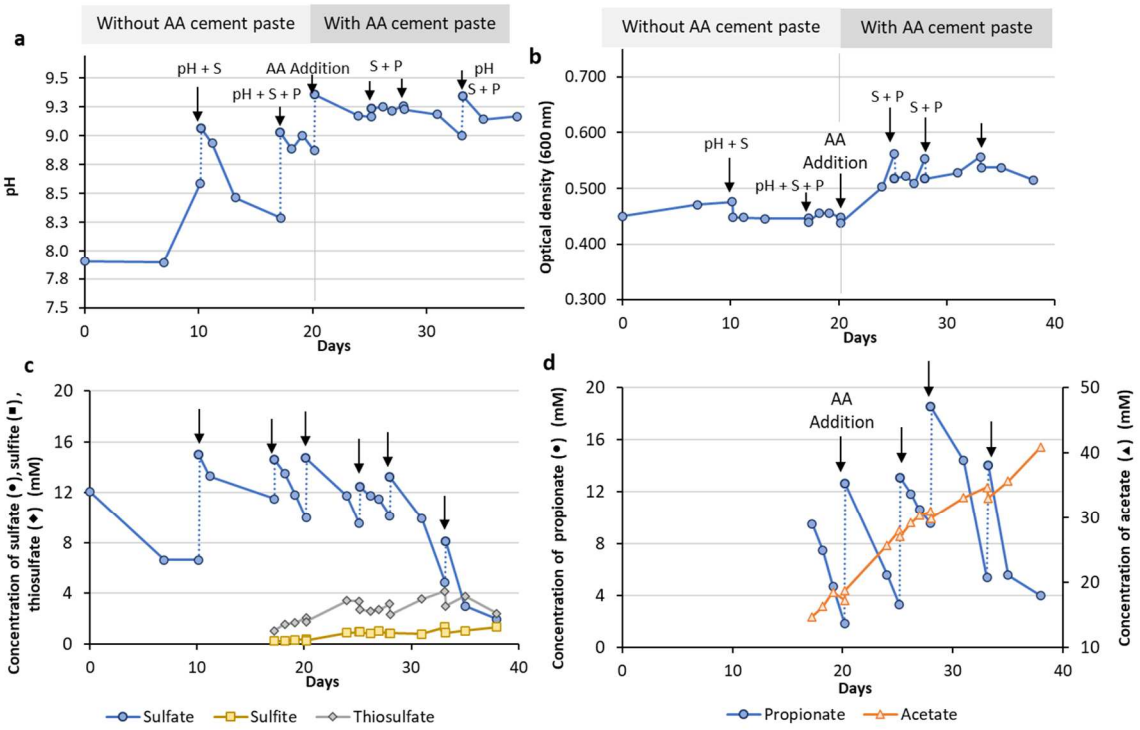

Figure 2: Evolution of the pH (a) and the Optical Density OD (b) within the bioreactors into which AA cement pastes coupons were incorporated on day 20 with a solid surface to liquid volume ratio of 71 cm^2/L. Variations in concentrations of sulfate, sulfite and thiosulfate (c), and propionate and acetate (d). The black arrows indicate incorporation of cementitious materials, sulfate (S) and propionate (P) additions, and pH adjustments.

During step 2, between days 17 and 20, the average OD was 0.450 in the bioreactor with an SA/V ratio of 71 cm^2/L. The sulfate was reduced to sulfite and thiosulfate, which reached the maximal concentrations of 0.4 mM and 2 mM, respectively, on day 20. Approximately 70% of the carbon from the propionate oxidation was converted into acetate and CO_2. Over all the bioreactors, the average SRR was 1.42 $\pm$ 0.13 mM/d and the average POR was 1.66 $\pm$ 0.58 mM/d, with an average pH of 9.1 (Table 2)

Immediately after the introduction of the AA cement paste coupons, an increase in pH from 8.9 to 9.4 was observed on day 20 (Figure 2.a). The same phenomenon was observed on day 33 immediately after bubbling. The OD increased steadily from 0.45 to 0.52 between days 20 and 26, probably due to precipitates formed in solution from the reaction between cementitious ions released by the AA cement paste coupons, then the OD remained constant between day 26 and day

39. The presence of solid cement pastes did not affect the OD significantly (Figure 2.b). Sulfate was reduced into thiosulfate and sulfite. Their concentrations increased and then stabilized after about 8 days to remain close to 0.9 mM of sulfite and 4.0 mM of thiosulfate (Figure 2.c). Figure 2.d shows propionate removal and the simultaneous formation of acetate that accumulated in the bioreactor; 71% of the carbon from the oxidation of propionate was used to form acetate.

Table 1 summarizes the rates of sulfate reduction and propionate oxidation for the bioreactors operated with different values of SA/V, before and after the addition of AA cement paste coupons. Regarding the effect of the SA/V ratio at pH 9.2, the SRRs corresponding to SA/V ratios of 46 and 71 cm^2/L, 1.44 and 1.54 mM/d, respectively. These ratio values were similar to the SRR obtained without AA cement paste coupons, 1.40 cm^2/L at pH 9.1 (Table 1). Nonetheless, the SRR decreased to the value of 0.9 mM/d in the bioreactor containing the SA/V ratio of 96 cm^2/L. The POR was also little affected by SA/V ratios of 46 and 71 cm^2/L – with a rate close to 2 mM/d, similar to that without cement paste – but the POR decreased to 1.4 mM/d for the reactor corresponding to the ratio of 96 cm^2/L. In order to evaluate the impact of pH on SRR and POR, the data obtained from the reactors with 46 cm^2/L as SA/V ratios were collected and the average SRR and POR were calculated for different pH values. This highlighted a decrease of the SRR for pH above 9.4: from 1.10 mM/d at pH 9.0 to 0.67 mM/d at pH 9.4, and also showed that the POR varied from 1.48 mM/d at pH 9.0 to 0.84 mM/d at pH 9.4.

Table 1: Sulfate reduction rate and propionate oxidation rate with and without AA cement paste coupons according to different SA/V ratios or according to different pH values.

	Solid/liquid ratio	Average initial pH*	POR (mM/d)	Acetate production rate (mM/d)	SRR (mM/d)
Without AA cement paste coupons - all reactors included (+ sd)		9.1 ± *0.0*	2.10 ± *0.40*	2.10 ± *0.90*	1.40 ± *0.10*
With AA cement paste coupons according to different solid/liquid ratios for the same pH **	46 cm^2/L	9.2	2.04	1.86	1.44
	71 cm^2/L		1.92	1.84	1.54
	92 cm^2/L		1.38	1.38	0.90
With AA cement paste coupons according to different pH values for the same SA/V (+ sd)	46 cm^2/L	9.0 ± *0.1*	1.48 ± *0.70*	1.10 ± *0.20*	1.42 ± *0.60*
		9.2	1.65	1.10	1.86
		9.4 ± *0.1*	0.84 ± *0.60*	0.67 ± *0.30*	0.82 ± *0.30*

* pH measured after supplementation and N_2 bubbling; ** standard deviation (sd) when the calculation is possible i.e. when there were more than three measuring points *** SRR: sulfate reduction rate; POR: propionate oxidation rate

3.1.2 Biological investigations

The investigation of microorganisms adsorbed onto, bound by or colonizing the surfaces of AA cement paste coupons was conducted by specific fluorescent labelling capable of revealing the presence of microbial cells by observation with epifluorescence optical microscopy (Figure S.7 in supplementary material). The cement paste surface was covered with rounded clumps, whose green fluorescence suggested that they were microbial clusters about 30 µm thick. Other filamentous structures, possibly corresponding to chains of microorganisms such as filamentous bacteria (Figure S.7**,** white rectangles), were also highlighted. These structures were quite distinct from calcite precipitates, which are sometimes capable of emitting auto-fluorescence under epifluorescence light microscopy (Chang et al., 2003; Durban et al., 2020).

At the end of step 3, in order to confirm the presence of microorganisms attached to the cement paste surface and to study their metabolic activity, the cement paste from one of the bioreactor with an SA/V ratio of 46 cm^2/L was transferred to a new bioreactor containing fresh cement leachate and

supplemented with sulfate and propionate according to the protocol described by Durban et al. (2020) (detailed protocol in supplementary data; section 1). A progressive increase of the OD (Figure S.8 in supplementary data) together with a reduction of sulfate and an oxidation of propionate (Figure S.8) confirmed that micro-organisms were indeed attached to the surface of the cement paste, because they were the only possible source of microorganisms in the bioreactor. The oxidation of propionate coupled with the reduction of sulfate increased with the recolonisation of the supernatant. Between days 8 and 15, a POR of 0.46 mM/d and SRR of 0.64 mM/d were reached while between days 15 and 21, a POR of 2.35 mM/d and SRR of 1.65 mM/d were was obtained.

The microbial populations that constituted the inoculum, i.e. activated sludge from domestic wastewater treatment plants, was similar to that described by Durban et al. (2020), i.e. the main phyla within the microbial community were *Proteobacteria* (≈20%), *Actinobacteria* (10%), *Planctomycetes* (9%), *Bacteroidete*s (5%), *Chloroflexi* (4%) and *Firmicutes* (3%) (Figure S.9 in supplementary material). A microbiological examination of the microbial community established close to the surface of the cement paste showed a dominance in the community of *Proteobacteria* (82%) and, more especially, of *Desulfomicrobium sp*. (80%). *Firmicutes* (2%) and *Spirochaetes* (2%) were present in lesser degrees.

3.1.3 Analysis of cement paste coupons

3.1.3.1 Macroscopic observations

The ageing process induced a dense cracking pattern on the surface of AA cement paste coupons (Figure S.11.a and b), probably due to chemical shrinkage following the intense leaching of calcium and other cementitious cations (creation of porosity) (Bertron et al., 2007). The cracks were still visible on the cement pastes after their 18 days' immersion in the bioreactor at pH 9.0. Moreover, the outer layer of the cement paste turned black, likely as a result of the formation of iron sulfide resulting from the reaction between iron leached from cementitious material and sulfide formed by the reduction of sulfate by SRB (Figure S.11.c and d).

3.1.3.2 Chemical and microstructural characterization of AA cement pastes coupons before and after their exposure in the bioreactors

- ***AA cement paste coupons before exposure:***

Figure 3 presents the SEM observation of an AA cement paste coupons after the pre-treatment with acetic acid and ultra-pure water (Figure 3.a) and its chemical composition profile (Figure 3.b) obtained with EDS.

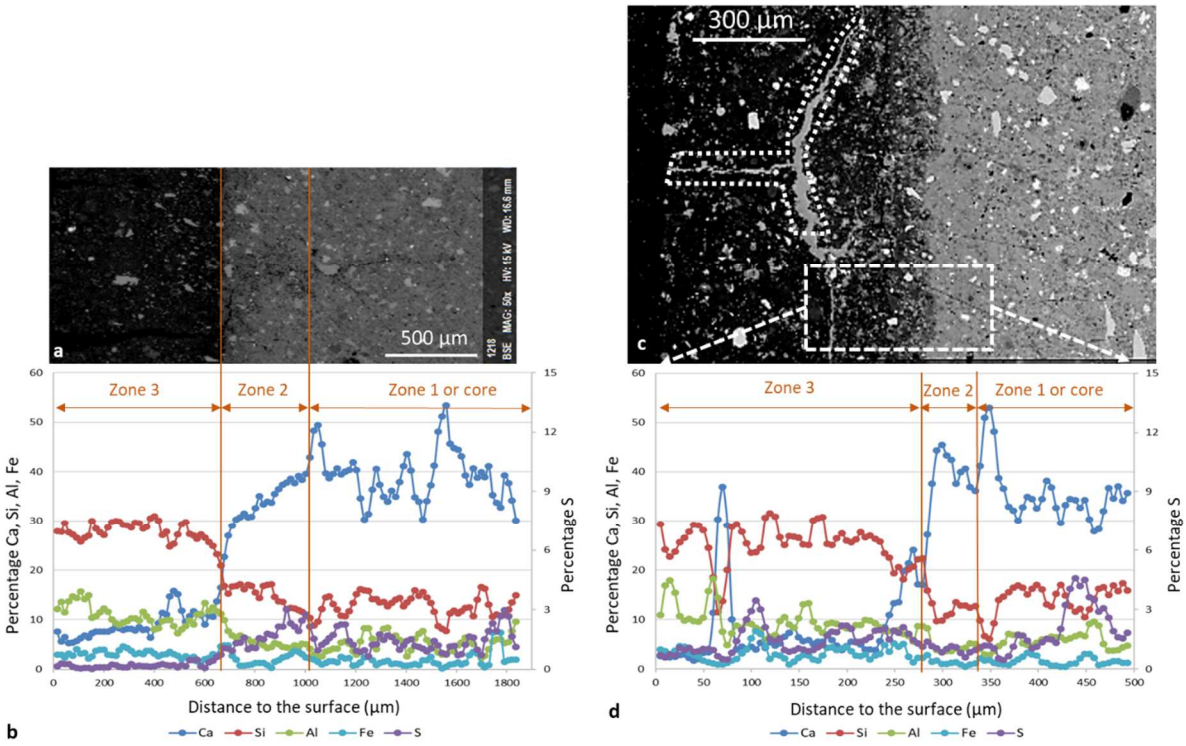

Figure 3: Scanning electron micrograph (SEM) of the external micrometres of a cross section of the AA cement paste coupon before (a) and after its exposure to the culture medium in the bioreactor with a ratio of 92 cm^2/L (c). Evolution of the chemical composition of the corresponding zones, mainly Ca, Si, Al, Fe, and S, according to the distance to the surface (b and d). Three different zones can be identified within the cross-section AA of the cement paste coupon: the core of the cement paste corresponds to zone 1 while the surface that was exposed to the bioreactor corresponds to zone 3. The area delimited in the upper left corner of the SEM image (b) corresponds to self-healing of the AA cement paste coupon, due to biological activity and calcite formation.

A chemical and microstructural zonation is clearly visible (the greyscale in SEM in backscattered electron mode depends on the intensity of the signal, and expresses the mass density of the matter). Zone 1, or the sound zone/core of specimen, has the typical composition of an unaltered

398 cementitious specimen. It is mainly composed of Ca (37.4 % on average), Si (14.6 %), Al (6.1%), Fe
399 (1.7%), and S (1.4%). It shows lighter grey residual anhydrous grains, embedded in a darker grey
400 hydrated cement matrix. Actually, the hydration of cementitious materials reduces the average
401 atomic number of the phases because of the water molecules integrated into the structure, and the
402 black zones correspond to porosity. Zone 2, which can be considered as a transition zone between
403 zones 1 and 3, is characterized by a progressive decrease of the Ca and S contents, together with a
404 relative increase of Si, Al and Fe contents. Residual anhydrous grains are still visible in this zone. The
405 limit between zone 2 and zone 3 is marked by a sharp decrease in the calcium content. Zone 3, the
406 outer layer exposed to the acid solution, is darker than zones 1 and 2, indicating a lower density of
407 the paste. This zone is indeed strongly decalcified (average Ca content 9.1 %) and S is completely
408 leached, whereas Si, Al and Fe have been preserved, as these elements were stable during the acid
409 attack carried out during the pre-treatment. The thicknesses of zones 2 and 3 are 670 µm and 340
410 µm, respectively, and the total altered layer thickness (zone 2 + zone 3) is 1010 µm.

411 • ***AA cement paste coupon after exposure***

412 Three main zones can be distinguished on the Figure 3.d according to the distance to the surface in
413 contact with the liquid medium. Zone 1 corresponds to the unaltered core of the specimen, while
414 zone 3 corresponds to the outer layer of the cement paste, including the surface exposed to the
415 microbial communities (Figure 3.c). Zone 1 has the typical microstructural, chemical and
416 mineralogical pattern of a sound hydrated cement paste. Zone 2, about 83 µm thick, is slightly
417 decalcified, showing a much lower density of anhydrous grains and no enrichment of sulfate (Figure
418 3.c and d). In zone 3, which is 750 µm thick, there is a progressive, but very strong, decrease of the
419 calcium content tending to zero in the outer layer (Figure 3.d). It is mainly composed of Si, Al, and Fe
420 (Figure 3.d). It is also noticeable that sulfur is still present in this zone although it was absent from
421 specimens exposed to pH 4 acetic acid solution (Figure 3.a and b). This may be due to an enrichment
422 of exogenous sulfur diffusing from the liquid phase of the bioreactor and precipitating in the
423 cementitious matrix. Additionally, a crack network filled with secondary precipitates is clearly visible.

Chemical analyses showed that these precipitates were composed of calcium, suggesting the formation of $CaCO_3$. This secondary precipitate is highlighted on the chemical composition profile: at 280 µm, a localized, strong increase in Ca is observed. This precipitation of calcite, clogging the cementitious matrix cracks, could be attributed to the microbial activity of SRB (Figure 3.c).

SEM imaging of the surface of cement coupons highlights the presence of sphere-shaped compounds (Figure S.10), a few micrometres in diameter, within some fractured zones of the AA cement pastes coupons (Figure S.10.a - b). The results of EDS analyses show that these spheres are composed mainly of calcium (Table S.3, spectra 1 (Figure S.10.a), 4 and 6 (Figure S.10.b)). According to the X-ray diffraction analyses (Figure S.12), these compounds on the surface of the materials were calcium carbonate precipitates ($CaCO_3$).

Other punctual chemical analyses on the surface of the cement coupons (Table S.3, spectra 3, 5, 7) highlighted that the matrix was mainly composed of silicon, aluminium and iron, confirming the strong decalcification of the matrix (because of the AA cement paste coupon pre-treatment). The sodium content was also noticeable – and unusual considering the pre-treatment. It may have been due to an enrichment by exogenous sodium (sulfate was introduced in the bioreactor in the form of sodium sulfate and propionate was neutralised with NaOH). This type of enrichment by exogenous sodium in the outer layer of decalcified cement paste has already been reported in the literature (Bertron et al., 2005a).

3.2 Assessment of the microbial propionate oxidation and sulfate reduction in the presence of moderate aged (MA) cement paste coupons

3.2.1 Analysis of the liquid fraction of the bioreactors

The SRR and POR were investigated in duplicate in the presence and absence of MA cement paste coupon for one SA/V ratio, 92 cm^2/L. Figure 4 presents the evolution of pH (a), OD (b), concentrations of sulfate, sulfite and thiosulfate (c), and the concentrations of propionate and acetate (d) in the liquid phase for one of the duplicates of the experiment (Reactor A). The results of the duplicate, the bioreactor B, are available as supplementary data (Figure S.13).

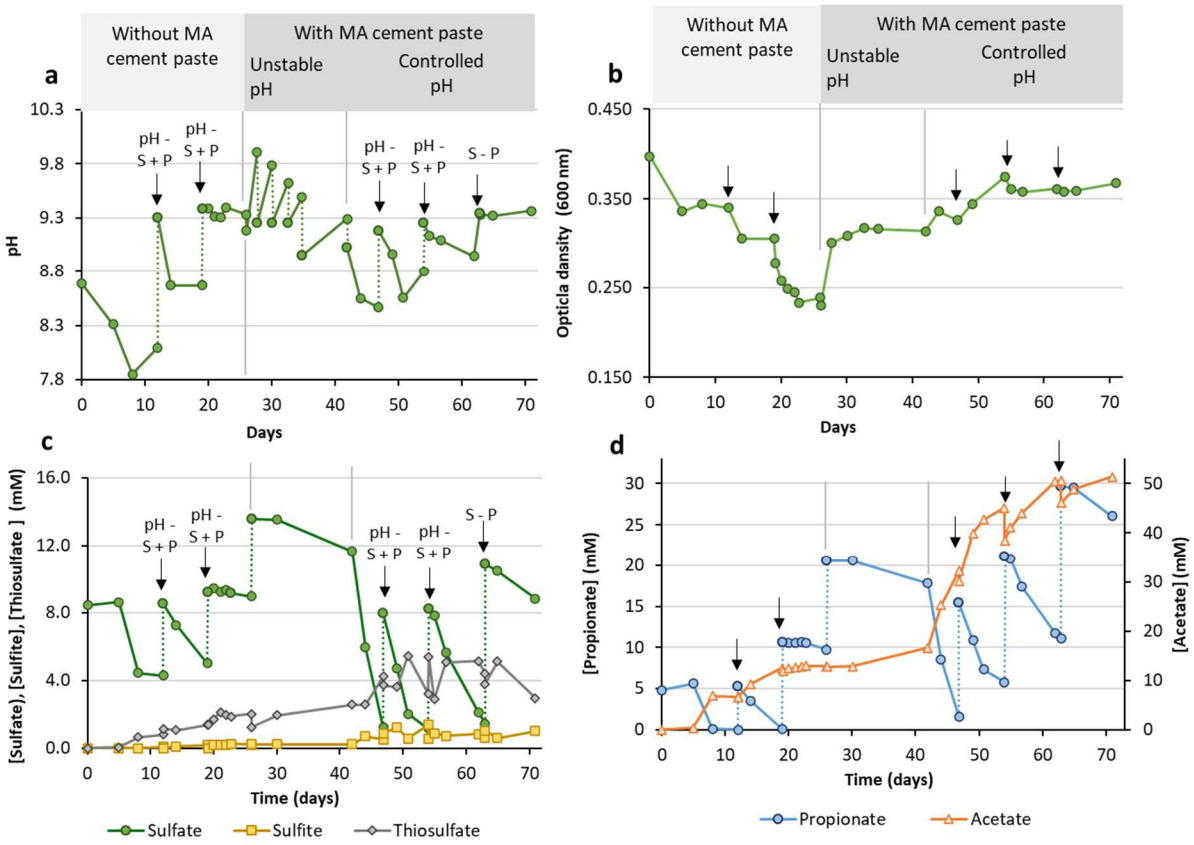

Figure 4: Evolution of pH (a), Optical Density (b), concentration of sulfate, sulfite, thiosulfate (c), propionate and acetate (d) in the bioreactor into which MA cement paste coupons were inserted at day 26, with a ratio of 92 cm^2/L. The black arrows indicate pH adjustment, and sulfate (S) and propionate (P) additions.

Three different steps can be distinguished, (i) the initial acclimation phase without solid cement paste and, jointly, evaluation of the PORs and the SRRs for several pH values (steps 1 and 2: days 0 to 26), (ii) the acclimation of SRB to the chemical conditions imposed by the MA cement pastes coupons added on day 26 (step 3a: days 26 to 42), and (iii) propionate oxidation coupled with sulfate reduction after SRB acclimation (Step 3b: days 42 to 71) (Figure 4).

During step 1, the pH decreased from 8.7 to 7.9 between days 0 and 8 (Figure 4.a) while sulfate reduction and propionate oxidation were only observed from day 5. Sulfate concentration decreased from 8.6 mM to 4.4 mM; it was reduced into sulfite (maximal concentration of 0.2 mM) and thiosulfate (maximal concentration of 2 mM). These reductions of the sulfate and the products from the sulfate reduction were coupled with the oxidation of propionate into CO_2 and acetate, which gradually accumulated in the bioreactor. On average, 76% of the carbon from the oxidation of

propionate led to the generation of acetate. A decrease in OD from 0.40 to 0.24 was observed between days 0 and 26 (Figure 4.b), due to the acclimation of microorganisms from activated sludge to the operating conditions in the bioreactor. Despite this, the biological propionate oxidation and the sulfate reduction was well established by day 12. Table 2 summarizes the SRR and POR for both bioreactors, before and after the addition of MA cement paste coupons. Before MA cement pastes coupons addition, at an average initial pH of 8.7 and 9.4, the SRR and POR decreased with the pH increase from 0.9 mM /d to 0.1 mM /d for SRR and from 1.3 mM/d to 0.1 mM/d for POR. The MA cement paste coupon addition induced an increase in pH to values around pH 10.0 on day 28 (Figure 4.a). This was due to the release of hydroxide ion from MA cement paste coupons. An increase of OD values from 0.23 to 0.30 also occurred, due the formation of precipitates resulting from the leaching of cement cations (Figure 4.b). Consequently, several pH balance corrections to pH 9.0 were performed during step 3a (days 26 to 42) to avoid excessive drift towards very alkaline pH levels detrimental to the viability of microorganisms. The pH then fluctuated between 8.8 (lowest value) and 9.9 (highest value). During step 3a and after day 28, the OD remained constant with an average value of 0.31. (Figure 4.a). Only a very slight reduction in the sulfate concentration was observed during this step with an SRR of 0.2 mM/d as well as a POR of 0.2 mM/d (Figure 4.a).

The OD increased slightly from 0.31 on day 42 to 0.35 on day 55 and remained constant thereafter (Figure 4.b). Associated with this increase in OD and as a consequence of the pH adjustment, the beginning of phase 3b was characterized by a decrease in pH over 5 days (from 9.0 to 8.5) associated with a significant reduction of sulfate (SRR of 2.21 mM/d) coupled with an oxidation of propionate (POR of 3.46 mM/d). This step (3b) corresponded to a stabilization of the pH and a significant biological activity of sulfate reduction and propionate oxidation, which followed a latent step (step 3a) where the instability of the pH was not favourable to such biological activity. This latent step lasted 16 days for the reactor A (Figure 4) and 28 days for the duplicate, reactor B (Figure S.13).

As previously observed, the sulfate reduction led to the formation of reactive intermediates that did not accumulate, i.e., sulfite and thiosulfate (Figure 4.c). The concentrations of sulfite and thiosulfate

reached were a little higher than in step 2 but of the same order of magnitude as for the experiments with AA cement paste coupon, i.e. an average 0.8 ± 0.3 mM for sulfite and 4.1 ± 1.0 mM for thiosulfate. On the other hand, acetate gradually accumulated in the system, resulting from the oxidation of propionate. 86% of the carbon from the oxidation of propionate was used to form acetate.

Table 2 reports the SRRs and PORs calculated for several pH values before the addition of MA cement pastes coupons and after their addition into the bioreactor at day 26. Before cement paste addition, the PORs decreased as the pH increased from 1.3 mM/d at pH 8.7 to 0.2 mM/d at pH 9.4, i.e. a decrease of 86%. This was also observed for the SRR, with a decrease of 89%. The impact of pH on POR and SRR was also observed after introduction of the cement paste and stabilization of the operating conditions (especially pH), with a decrease in POR of 83% (2.9 at pH 9.0 and 0.5 mM/d at pH 9.4) and a decrease of 84% for SRR (1.9 mM/d at pH 9.0 and 0.3 mM/d at pH 9.4).

Table 2: SRR and POR calculated at different pH measurements with a ratio of 92 cm^2/L, for the bioreactor before the addition of MA cement pastes, and after their addition into the bioreactor. The initial pH value corresponds to the first pH measurement at the beginning of the experiment.

	Solid/liquid ratio	Average initial pH*	POR	Acetate production rate	SRR
			(mM/d)	(mM/d)	(mM/d)
Without MA cement paste coupon - all reactors included (+ sd)		8.7 ± *0.0*	1.3 ± *0.8*	0.8 ± *0.1*	0.9 ± *0.6*
		9.3 ± *0.0*	0.8 ± *0.1*	0.9 ± *0.1*	0.5 ± *0.1*
		9.4 ± *0.0*	0.2 ± *0.1*	0.1 ± *0.1*	0.1 ± *0.1*
With MA cement paste coupon all reactors included (+ sd)**	92 cm^2/L	9	2.9	2.8	1.9
		9.2	1.5	2	1.1
		9.3 ± *0.0*	1.1 ± *0.8*	1.4 ± *0.9*	0.8 ± *0.6*
		9.4	0.5	0.4	*0.3*

* pH measured after supplementation and N_2 bubbling; ** standard deviation (sd) when the calculation is possible i.e. when there were more than three measuring points *** SRR: sulfate reduction rate; POR: propionate oxidation rate

3.2.2 Biological investigations

3.2.2.1 Presence of bacteria attached to the surface

In order to confirm the presence of microorganisms attached to the surface and to study their metabolic activity independently of the planktonic fraction (microorganisms in the supernatant), at

514 the end of step 3 for the experiment with MA cement paste coupons, one cement coupon of each
515 bioreactor was transferred into a new bioreactor containing cement leachate supplemented with
516 sulfate and propionate. This experiment was therefore conducted in duplicate (section S.1 in
517 supplementary data). Before any biological activity, growth or redox reaction could be observed,
518 over the two bioreactors, a transitional period before pH stabilisation of the order of one hundred
519 days with a frequent pH adjustment (once or twice a week during the first fifty days) was necessary.
520 This strong increase of the pH resulted from a release of the hydroxide ions still present in the
521 cement paste (Figure S.2). After this acclimatization period, the OD increased slowly and reached the
522 maximal value of 0.2 after 175 days. Then a significant reduction of the sulfate associated with an
523 oxidation of the propionate into acetate and CO_2 was observed (Figure S.14). On average, the SRRs
524 observed were 0.7 $\pm$ 0.2 mM/d and the PORs were 1.1 $\pm$ 0.3 mM/d for an average pH of 8.8.

525 A recolonization of the supernatant by microorganisms reducing the sulfate and oxidizing the
526 propionate was established. The cement paste being the only source of microorganisms, the
527 presence of bacteria attached to the surface was most likely.

528 Therefore, at the end of this experiment, microscopic observations were performed: epifluorescence
529 microscopy observations on the cement surface after DNA labelling by Syto 9, and SEM observations
530 (Figure 5). Both techniques revealed bacteria adhered to the surface of the MA cement paste coupon
531 around the calcite precipitates (Figure 5). EDS analyses (data not shown) detected phosphorus in
532 spherical structures. The morphology of which also observed in Figure 5.b, suggested that they were
533 bacteria.

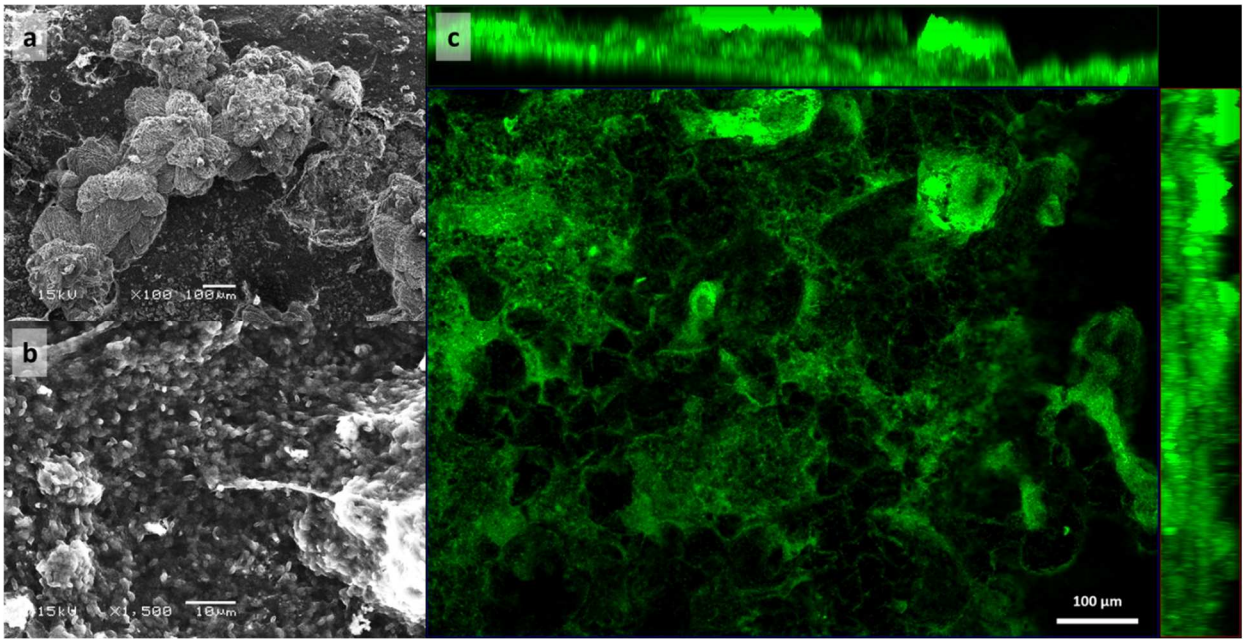

Figure 5: SEM (a,b) and epifluorescence microscopic imaging (c) with Syto 9 labelling of an MA cement paste after 180 days of immersion in the bioreactor after renewal of the culture medium by cement leachate enriched with sulfate and propionate.

3.2.2.2 Evolution of bacterial communities

The microbial populations from the inoculum and present in the bioreactor were identified by molecular inventory of 16S rRNA (see section S.2 and Figure S.9 in supplementary data). The analysis of the microbial populations from the inoculum, i.e. activated sludge, showed that the main phyla within the microbial community of the inoculum were Proteobacteria (≈20%), Actinobacteria (10%), Planctomycetes (9%), Bacteroidetes (5%), Chloroflexi (4%) and Firmicutes (3%) (Figure S.8).

Before MA cement paste coupon addition, the community was dominated by three phyla: *Proteobacteria* (26%), *Firmicutes* (29%) and *Chlorob*i (22%). The phylum *Proteobacteria* was mostly represented by the class *Deltaproteobacteria* (11.5%) of which the genus *Desulfobulbus* was present at 5 % and the others were unknown. The genus *Candidatus Competibacter* made up 6% of the class *Gammaproteobacteria* and the remaining 8% corresponded to species belonging to the orders Burkholderiales, Rhodobacterales and Rhizobiales, having less than 1% representability. The phylum *Firmicutes* (29%) was represented by *Fusibacter* (27%) and the phylum *Chlorob*i (22%) was represented by *Ignavibacterium*.

After 71 days of culture, 45 of which in the presence of MA cement paste coupon, the community was dominated by the phylum *Proteobacteria* (83%), especially the species *Desulfomicrobium sp.* The medium was then renewed with fresh cement leachate supplemented by sulfate and propionate. The supernatant was recolonized after 180 days of culture. This population was analysed but 51% of the sequences obtained could not be characterized. The other sequences were mostly attributed to the phylum *Proteobacteria* (45%), especially the species *Desulfomicrobium sp*.

3.2.3 Analysis of the cement coupons

3.2.3.1 Macroscopic observations

Compared to the advanced ageing protocol, the moderate ageing process did not visibly fracture the surfaces of the MA cement paste coupons, which maintained a homogenous light grey pattern (slightly lighter tint than that of a sound specimen) (Figure S.11.e). However, dark spots were noticed on cement paste surfaces after 45 days of immersion in the bioreactors enriched with sulfate-reducing and propionate-oxidizing bacteria (Figure S.11 f).

3.2.3.2 Chemical and microstructural characterization of MA cement pastes coupons before and after their exposure in the bioreactors

- ***MA cement paste before exposure:***

Figure S.15 in the supplementary data presents SEM observations (Figure S.15.a) and a chemical composition profile (Figure S.15) obtained with EDS of an MA cement paste coupon after the moderate ageing (MA) protocol with pure water. The analyses reveal a much less intense deterioration pattern induced by the moderate ageing process (Figure S.15) compared to the advanced ageing process (Figure 3). Two zones were visible: zone 1 or the core of the specimen, where the average calcium content was 34.8%, and zone 2, only slightly decalcified: the content of Ca was 28.6% in this zone. The average sulfur (S) content in zone 1 was 1.8%, but it dropped to 0.4% in zone 2. Si, Al and Fe were preserved in this zone, which had a thickness of about 150 µm.

- ***MA cement paste coupon after exposure to the bioreactor:***

The SEM imaging of the cross section of MA cement paste coupon after 45 days of immersion in the bioreactor allowed three different zones to be distinguished (Figure 6.b).

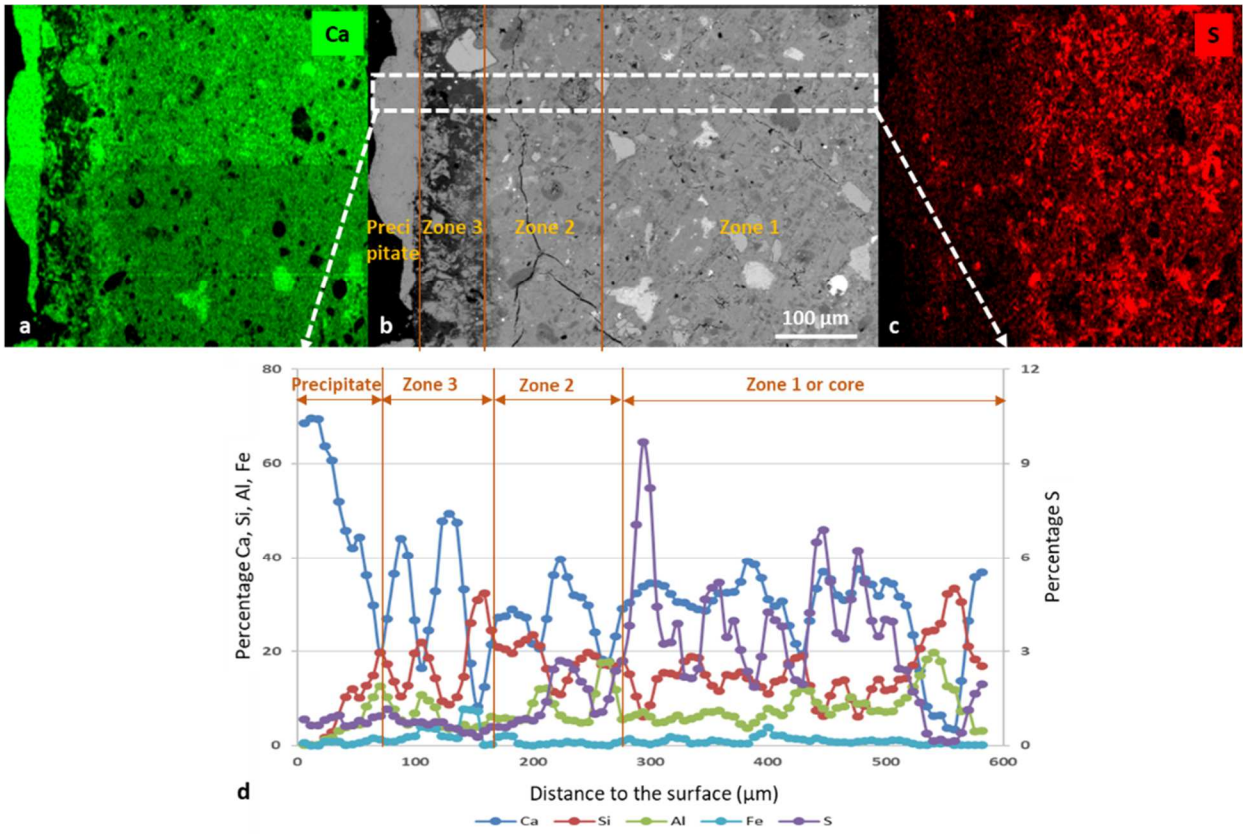

Figure 6: Scanning electron micrograph (SEM), in backscattered electron mode, of the external layer from the cross section of a MA cement paste coupon that was immersed for 45 days in the bioreactor (b), and EDS mapping of the calcium content in green (a) and sulfur content in red (c). In (d), evolution of the chemical composition (Ca, Si, Al, Fe, and S) of zones 1, 2, 3 and 4 identified according to the distance to the surface of MA cement paste coupons. Zone 1 corresponds to the core of the MA cement paste, while zone 3 corresponds to its surface that was exposed to the microbial communities.

The microstructural, chemical and mineralogical patterns of zone 1 correspond to those of a sound hydrated cement paste. Zone 2, with a thickness of 110 µm, contained fewer anhydrous grains, but the average density of the hydrated matrix seemed equivalent to that of zone 1. Coupling these results with EDS analysis determined that the calcium contents in zones 1 and 2 were similar (27.7% and 28.36 %, respectively) (Figure 6.a). The calcium content decreased considerably at the limit between zone 2 and zone 3 and reached 10.5%, due to Ca leaching from the cement paste. Despite the ongoing process of calcium leaching from MA cement paste coupons, the calcium content in zone

598 3, although irregular, was high. This higher calcium content could have resulted from the microbial
599 activity of the SRBs in the bioreactor (Figure 6.a), whose CO_2 production could have reacted with the
600 Ca released from the pulp and led to the precipitation of $CaCO_3$ in this area. EDS Ca mapping (Figure
601 6.a), SEM observation in back-scattered electron mode (Figure 6.b), and the EDS profile (Figure 6. d)
602 highlighted the presence of a precipitate a few tens of µm thick and mainly composed of calcium on
603 the surface of the coupon, likely a $CaCO_3$ precipitate according data obtained by XRD (data not
604 shown). Regarding the fate of sulfur, the average content of this element in zone 1 was 3.1%. It
605 decreased in zone 2 and even more near the surface (zone 3) but EDS S mapping showed areas with
606 local enrichment in sulfur, even close to the surface (Figure 6.c). The SEM imaging coupled to EDS
607 analyses highlighted several cracks with such localized sulfur enrichment (Figure 6.b, c, and in
608 supplementary data S.16 with the Table S.4). Their microstructure suggested the presence of
609 secondary expansive ettringite, which could explain the sulfur enrichment. In zone 3, the sulfur
610 content stabilized around 1.1%. The presence of sulfur in zone 3, as well as the precipitation of
611 secondary ettringite in zone 2, could be related to a diffusion of exogenous sulfur present in the
612 bioreactor. The total thickness of zones 2 and 3 was about 210 µm.
613 SEM imaging coupled with EDS analysis of the surface of the specimens highlighted several calcium-
614 rich precipitates with different morphologies and sizes from ten to a hundred µm (Figure S.17 and
615 Table S.5 in supplementary data), suggesting the presence of calcium carbonate precipitates ($CaCO_3$).
616 Other punctual chemical analyses performed on the cement paste surface (Table S.5) revealed
617 compounds mainly composed of aluminium and silicon, which probably correspond to silico-
618 aluminous fly ash contained in CEM V cement.

619 **4 Discussion**

620 **4.1 Bio-reactivity of sulfate and propionate**

621 For a pH close to 9.0, with or without cement paste, the propionate was oxidized into CO_2 and
622 acetate, which accumulated in the bioreactor. The oxidation of the propionate was incomplete; i.e.,
623 propionate was not completely oxidised to CO_2, an average of 74% of the oxidized carbon being

transformed into acetate. Moreover, the presence of sulfite and thiosulfate, two intermediate forms of sulfate reduction, was observed. According to the sulfate reduction pathway, coupled with the oxidation of propionate, sulfate was first reduced to sulfite (reaction 1 below) which was reduced to sulfide (reaction 2) or to thiosulfate, which is an intermediate step in sulfite reduction (reactions 3 and 4) (Bradley et al., 2011; Qian et al., 2019). The global reaction of the sulfate reduction to sulfide coupled to the oxidation of propionate is described by reaction 5 at pH close to 9.0, with HS^- as major form of hydrogen sulfide (Widdel and Pfennig, 1981):

$C_3H_5O_2^- + 3\,SO_4^{2-} \rightarrow 3\,SO_3^{2-} + H^+ + HCO_3^- + C_2H_3O_2^-$ (1)

$C_3H_5O_2^- + 3\,SO_3^{2-} \rightarrow HS^- + HCO_3^- + C_2H_3O_2^-$ (2)

$C_3H_5O_2^- + 3\,SO_3^{2-} + 2\,H^+ \rightarrow 1.5\,S_2O_3^{2-} + 1.5\,H_2O + HCO_3^- + C_2H_3O_2^-$ (3)

$C_3H_5O_2^- + 0.75\,S_2O_3^{2-} + 0.75\,H_2O \rightarrow 1.5\,HS^- + H^+ + HCO_3^- + C_2H_3O_2^-$ (4)

$C_3H_5O_2^- + 0.75\,SO_4^{2-} \rightarrow 0.75\,HS^- + 0.25\,H^+ + HCO_3^- + C_2H_3O_2^-$ (5)

According to the redox reactions, the reduction of sulfate to sulfite (reaction 1) or thiosulfate to sulfide (reaction 4) leads to a production of proton (H^+) which can lead to a decrease in pH. This was indeed observed during the reduction of sulfate in the different reactors with and without cement paste. On the other hand, the reduction of sulfite to thiosulfate requires a consumption of protons (reaction 4), which, in an alkaline environment, can be a limiting step of the sulfate reduction due to the low (bio) availability of H^+.

Before the addition of AA or MA cement paste coupons, the PORs were between 1.3 and 2.1 mM/d at pH close to 9.0 and the SRRs were between 0.9 and 1.4 mM/d. However, the increase of the pH induced a decrease in the PORs and SRRs similar to an inhibiting effect, especially for pH values above 9.3: the POR decreased by 89 % and the SRR by 85% when the pH increased from 8.7 to 9.3 without cement paste. With MA cement paste coupons (Table 2), both the SRRs and the PORs decreased by 20% for each pH increase of 0.1, between 9.0 and 9.3, which represented an overall decrease of 62% for POR and 68% for SRR for a pH increase from 9.0 to 9.3. For pH higher than 9.3,

650 the SRRs and PORs decreased, respectively, by 83% and 84% compared to the values obtained at pH
651 9.0 and no significant sulfate reduction was observed for pH above 9.5. Other studies have also
652 noted a poor reduction of sulfate at pH values above 10 and have defined a critical pH value of 9.3
653 above which sulfate reduction is strongly affected (Goeres et al., 1998; Rizoulis et al., 2012). In the
654 case of AA cement paste coupons addition, the pH impact on the PORs and SRRs was also observed
655 but was more moderate. The rates decreased by 43% for POR and 39% for SRR for a pH increase from
656 9.0 to 9.4. This can be explained by the higher level of alteration of AA cement paste coupons and
657 the presence of lower SA/V ratio, and therefore a lower alkaline cation and hydroxide reserve.

658 The propionate oxidation and sulfate reduction process together with the associated ratios, PORs
659 and SRRs, were little impacted by the addition of cement paste once the pH was stabilized and the
660 microbial activity in place for SA/V ratio below 96 cm^2/L. An increase in residual thiosulfate was
661 observed in the liquid phase, with an average concentration of 4 mM, i.e. twice as high as before the
662 cement paste addition. However, the addition of AA type cement paste coupons with a SA/V ratio of
663 96 cm^2/L had an impact on SRRs and PORS by inducing a decrease of about 35% compared to the
664 performance obtained without cement paste. The PORs and SRRs obtained at pH 9.2 with a SA/V
665 ratio of 92 cm^2/L were similar between experiments with AA and MA cement paste coupons.
666 Moderate ageing of the cement paste delayed the emergence of microbial activity by inducing a
667 strong increase in the pH of the medium, but once the pH stabilized and the microbial activity
668 established, the ageing of the cement paste did not strongly affect PORs or SRRs at pH 9.2.
669 Concerning models of the geochemical evolution of storage, these data will allow us to define the
670 conditions in which an oxidation of the organic matter coupled with the reduction of the sulfate
671 could be included in the geochemical equations used for the safety evaluation (Bagaria et al., 2021) ,
672 for pH lower than 10 or 9.5 and after alteration of the cement matrix. Moreover, the ability to specify
673 a pH threshold above which no microbial activity, thus no sulfate reduction nor organic matter
674 oxidation, occurs is essential. In sum, propionate oxidation and sulfate reduction was strongly slowed
675 down for pH higher than 9.3 and was not observed for pH above 9.5.

676

677 **4.2 Cement paste pre-treatment**

678 The AA cement paste coupons process induced strong alteration that was expressed by cracking of
679 the outer layer and a marked chemical and microstructural zonation. The deterioration patterns
680 were typical of the alteration of cement pastes exposed to acetic acid (Bertron et al., 2005b;
681 Duchesne and Bertron, 2013) with a fast leaching of calcium (Ca^{2+}), hydroxide (OH^-) and alkaline (Na^+,
682 K^+) ions without promotion of any secondary precipitation or any specific interactions between the
683 acetate anion (CH_3COO^-) and the cations leached from cement pastes (Bertron et al., 2007, 2005a,
684 2005b; Bertron and Duchesne, 2013). The outermost zone was strongly decalcified. This intense
685 leaching of calcium caused chemical shrinkage that resulted in the dense cracking pattern of the
686 outer layer, visible on the cement paste surface (Bertron et al., 2007).
687 The moderate ageing (MA) process, which consisted of one week leaching of the cement paste with
688 ultrapure water, induced much less intense alteration of the cementitious specimens, and thus
689 higher pH after their introduction into the microbial medium. The specimens maintained a
690 homogeneous light grey pattern close to that of a sound specimen, without any visible cracks. The
691 depth of alteration (150 µm) was almost ten times less than that of the AA cement paste coupons
692 and the chemical composition of the cement paste in contact with the liquid medium was little
693 affected by the leaching (slight decalcification and sulfur leaching).

694 **4.3 Impact of biological activity on solid matrices**

695 The exposure of the cement pastes to microbial activity, which catalysed the reduction of sulfate to
696 sulfide coupled with an oxidation of propionate to HCO_3^- and acetate, induced strong interaction
697 between microorganisms and cementitious material. These interactions led to an increase in the
698 degradation front depth of the outer layer with respect to the initial states of the AA and MA cement
699 paste coupons after their pre-ageing treatment, particularly for the AA pastes, which were initially
700 the most altered. For the AA cement paste coupons, the depth of degradation to the outer layer was
701 670 µm after pre-treatment and increased to 750 µm after exposure to the biological activity of

propionate oxidation and sulfate reduction whose reaction induced a production of sulfide and carbon dioxide. The specimen outer layer was progressively decalcified and the calcium content dropped to zero at the surface of the AA cement paste (vs. 8% Ca at the surface of AA paste after the pre-ageing process). The intensified decalcification of the AA cement paste coupons in the already altered zones may have been the consequence of aggressive chemical species produced by the SRB, notably the protons or acetate associated with the sulfate reduction and propionate oxidation (reactions 5), which induced an additional acid attack on the matrix (Magniont et al., 2011; Voegel et al., 2019b, 2016).

The presence of black spots or black stains was observed on AA cement pastes coupons surface after 18 days of immersion, and after 45 days on MA cement paste surface. Theses black spots might have been due to the precipitation of iron sulfide minerals resulting from the reactions between Fe(II) of the cement paste and sulfide formed by the microbial reduction of sulfate in solution (Amen et al., 2018; Etim et al., 2021).This reaction seems to have been more marked in the case of AA cement pastes coupons because of their higher level of alteration, which may have facilitated access to the ferrous sites.

In the transition zone between the outer layer exposed to the medium and the sound core of the cement paste, the presence of several cracks containing S, Ca and Al was observed for the MA cement pastes coupons. This is typical of secondary expansive ettringite precipitation, which may have occurred by reaction of exogenous non-reduced sulfate, diffused from the microbial medium through the outer zone, with calcium aluminate phases in the cement matrix (Menéndez et al., 2013).

Noticeable secondary precipitation of Ca-rich minerals was also observed in the outer layer and/or on the surface of AA and MA cement paste coupons exposed to SRB activity. A crack network sealed by calcium-rich secondary precipitates (mostly $CaCO_3$) was observed in the altered zone of AA cement paste coupons. Moreover, Ca-rich precipitates with different morphologies and sizes (from ten to a hundred µm), typical of calcium carbonates, were also observed on the surface of the AA

728 and MA cement paste coupons. The precipitation of $CaCO_3$ in the cracks and on the surface can be
729 viewed as self-healing by microbial induced calcium carbonate precipitation, which has been widely
730 studied in other contexts (Ersan et al., 2018; Joshi et al., 2017; Vijay et al., 2017). It occurs from the
731 reaction of the Ca leached from the cement matrix with the microbially produced CO_2. Actually,
732 bacterial walls, being negatively charged, have a strong affinity for nearby cations, including calcium
733 (Ca^{2+}), which tend to bind to their cell walls (Vijay et al., 2017). Ca^{2+} ions react with CO_2 produced by
734 the microbial oxidation of organic matter during sulfate reduction and then generate calcite
735 precipitation around the bacterial cell surface, which serves as a nucleation site (Ersan et al., 2018;
736 Joshi et al., 2017). The formation of calcium carbonate precipitate, in the polymorphic form of calcite
737 or aragonite, by sulfate-reducing bacteria has been observed previously (Hammes and Verstraete,
738 2002; Joshi et al., 2017) and the following reactions (2), with methanol as electron donor, and (3)
739 have been described by Peckmann et al. (1999):

740 $$2\,CH_2OH + SO_4^{2-} \longrightarrow H_2S + 2\,HCO_3^- \quad (2)$$

741 $$Ca^{2+} + HCO_3^- \longrightarrow CaCO_3 + H^+ \quad (3)$$

742 In the case of propionate oxidation to acetate, only one molecule of bicarbonate was produced
743 (Reaction 5). Thus, for each molecule of propionate oxidized, one molecule of calcium was consumed
744 and, theoretically, one molecule of calcite was produced.
745 Microbial colonization sites on solid materials are usually preferentially located in areas with good
746 bio-receptivity, where surfaces are less chemically and pH aggressive and are rough enough to
747 provide protection from an external environment that may be chemically or mechanically aggressive,
748 while ensuring good access to the substrate, (Flemming and Wingender, 2010; Voegel et al., 2016).
749 Based on these criteria, the initial bacterial adhesion, at the origin of the biofilm formation, could
750 preferentially take place on weathered areas or in cracks. This colonization and localized high
751 concentrations of SRB can lead to accelerated deterioration (such as calcification) due to the
752 production of aggressive metabolites. However, it can also lead to a consolidation of these areas by
753 precipitation of calcium, in the form of calcite, within the cracks or by forming a protective layer of

754 calcite on the surface. This would limit the subsequent diffusion of residual calcium from the paste to
755 the outside.
756 In the context of geological storage, a catalysis of sulfate reduction coupled with an oxidation of the
757 organic matter is assumed. These reactions could lead to a production of sulfides, organic acids (e.g.
758 acetate) and/or CO_2, thus acidifying the system and inducing an attack of the cement materials.
759

760 **4.4 Cement paste colonisation by microorganisms**

761 The analysis of the microbial population before the introduction of MA cement pastes coupons has
762 indeed enabled the identification of bacterial species belonging to the genus *Desulfobulbus*,
763 *Competibacter*, *Ignavibacterium* and *Fusibacter*. The species belonging to the genus *Desulfobulbus*
764 *sp.* are known to be SRB that use propionate as an electron donor and a carbon source to produce
765 and reduce thiosulfate (El Houari et al., 2017; Sorokin et al., 2014; Widdel and Pfennig, 1981). Some
766 species, such as *Desulfobulbus alkaliphilus sp.,* are obligately alkaliphilic and grow at pH 8.2 – 10.2
767 with an optimum at pH 9.4 (Sorokin et al., 2012). Concerning the species from the genus *Fusibacter*,
768 *Competibacter* or *Ignavibacterium*, little information about their role in the sulfate reduction process
769 is available in the literature. Some species from the genus *Ignavibacterium* have been reported as
770 versatile and able to reduce sulfate, e.g. *Ignavibacterium album* (Lino et al., 2010). No *Fusibacter* has
771 been reported to be involved in sulfate reduction but some species may participate in sulfite or
772 thiosulfate reduction and can thus be considered as alkaliphilic bacteria; i.e. bacteria that can live
773 and thrive in an alkaline environment with pH ranging from 8.5 to 11. (Liu et al., 2021; Ravot et al.,
774 2015).
775 In addition to the microbial population present in the liquid phase, the population of microorganisms
776 adhered to the surface of the cement paste has also been investigated. The presence of
777 microorganisms attached to the surface of the cement paste has been confirmed by microscopic
778 observation (epifluorescence and SEM) and experimentally (transfer of the cement paste in contact
779 with the inoculum into a fresh medium without microorganism (Durban et al., 2020)). The coverage

780 rate or the surface area colonized by microorganisms according to the different levels of cement
781 paste ageing (MA or AA cement paste coupons) could not be studied. However, the time required to
782 observe biological activity after transferring the cement pastes to a new reactor: 55 days for MA
783 cement paste coupons versus 1 day for AA, suggests that the AA cement paste coupons were more
784 easily and/or densely colonized than the MA cement pastes. The latter, less altered, released more
785 alkaline ion and hydroxide, imposing a pH that was not favourable to the growth and biological
786 activity of SRB. Whatever the degree of alteration and the culture time, the same species was
787 identified at the end of the experiments: *Desulfomicrobium sp*.. *Desulfomicrobium sp*. is a SRB that
788 grows in anaerobic environments and uses sulfate or sulfoxyanions as terminal electron acceptors,
789 producing H_2S, coupled with the oxidation of simple organic compounds such as lactate or
790 propionate, whose oxidation is, in some cases, incomplete and produces acetate as well as CO_2
791 (Genthner and Devereux, 2015). This SRB strain catalyses sulfate reduction under pH close to 8.5, i.e.
792 less sensitive to moderately alkaline pH than other SRB, such as *Desulfovibrio sp.* – a frequently
793 occurring SRB better adapted to reducing sulfate under acidic or neutral environments (Zheng et al.,
794 2014). Several works by Sorokin et al. (2015, 2014) have shown that some SRBs from soda lakes, such
795 as *Desulfonatronum sp.*, *Desulfonatronovibrio sp.* or *Desulfobulbus sp., could,* in the presence of
796 propionate, reduce sulfate at pH close to 11. However, these species were not selected in the
797 context of our study, although *Desulfobulbus sp.* was identified in the liquid phase before the
798 introduction of the MA cement paste. The addition of AA and MA cement paste coupons into the
799 bioreactor provided a niche environment for the SRB community to establish colonies or biofilm
800 within the altered surfaces.

801 Increasing the SA/V ratio increases the surface area available to microorganisms to develop and
802 would therefore promote microbial activity (growth and redox reaction) and the alteration of
803 cementitious materials. Furthermore, due to the leaching of cementitious materials, the increase in
804 the SA/V ratio will also favour an alkalinisation of the environment with more alkaline pH values,
805 which will have a limiting impact on biological activity. There are therefore several competing

phenomena. This study has shown that colonisation of the material is slow but seems to be favoured when the cementitious materials are altered. After transferring the cementitious material into a new reactor, on the one hand a recolonisation of the supernatant was observed and on the other hand it took at least 15 days of cultivation to reach SRR and POR comparable to the initial reactor. Thus, there were active microorganisms on the cement matrix.

5. Conclusion

This study highlights the possible organic matters oxidation, such as propionate coupled with the sulfate reduction by microbial activities for cementitious systems comparable to those found in nuclear waste cells. The use of different ratios of solid cement paste surface area to liquid volume generated different pH value and in different cementitious environments to be investigated. To mimic short-term and long-term cement ageing in the nuclear waste repository, moderate ageing (MA) and advanced ageing (AA) techniques were applied. The study allowed to determine the sulfate reduction and propionate oxidation rates at different pH values – around 1.6 and 1.4 mM SO_4^{2-}/d and 1.8 and 2.1 mM propionate/d at pH close to 9.0, with or without cement paste, respectively. It also highlights the strong decrease of the sulfate reduction/propionate oxidation rate with increasing pH: i.e. for a pH increase from 9.0 to 9.4 a decrease of 22% and 84% with AA and MA cement pastes coupons, respectively, and for a pH increase from 8.7 to 9.4 a decrease of 89% without cement paste. No sulfate or propionate oxidation was observed for pH above 9.5. The presence of microorganisms attached to the surface of cement pastes has been confirmed. This presence induced strong biogeochemical interactions between microorganism and cementitious material : microbial activity near the surfaces of solid materials led not only to alterations such as decalcification and sulfide enrichment with the appearance of secondary ettringite, particularly on MA pastes, but also to a relocation of calcium in the form of calcite either within the micro-fracture (AA cement paste coupons) or on the surface of the material (MA cements paste coupons) comparable to self-healing phenomena.

Acknowledgments

This research project was financially supported by the French national radioactive waste management agency (Andra) and by the University of Toulouse. The authors are grateful to S. Becker for improving the English language and to Agathe Juppeau for her technical support.

Credit authorship statement

Nadège Durban: Conceptualisation, Methodology, Investigation, Validation, Formal analysis, Writing - Original Draft, Writing - Review & Editing, Visualization.

Alexandra Bertron: Conceptualisation, Methodology, Ressources, Writing - Original Draft, Writing - Review & Editing, Supervision, Project administration, Funding acquisition.

Vanessa Sonois-Mazars: Validation, Investigation.

Maud Schiettekatte: Validation, Investigation.

Gerald Matar: Writing - Review & Editing.

Pierre Albina: Methodology, Validation.

Achim Albrecht: Conceptualisation, Supervision, Writing - Review & Editing

Jean-Charles Robinet: Conceptualisation, Project administration

Benjamin Erable: Conceptualisation, Methodology, Ressources, Supervision, Writing - Review & Editing Project administration

References

Abrahamsen, L., Arnold, T., Brinkmann, H., Leys, N., Merroun, M., Mijnendonckx, K., Moll, H., Polvika, P., Ševců, A., Small, J., Vikman, M., Wouters, K., 2015. A Review of Anthropogenic organic Wastes and Their Degradation Behaviour. Microbiol. Nucl. Waste Dispos. (MIND deliverable D1.1.).

Albina, P., Durban, N., Bertron, A., Albrecht, A., Robinet, J.-C., Erable, B., 2021. Nitrate and nitrite bacterial reduction at alkaline pH and high nitrate concentrations, comparison of acetate

versus dihydrogen as electron donors. J. Environ. Manage. 280, 111859. https://doi.org/10.1016/j.jenvman.2020.111859
Albrecht, A., Bertron, A., Libert, M., 2013. Microbial Catalysis of Redox Reactions in Concrete Cells of Nuclear Waste Repositories: A Review and Introduction, in: Bart, F., Cau-di-Coumes, C., Frizon, F., Lorente, S. (Eds.), Cement-Based Materials for Nuclear Waste Storage. Springer New York, New York, NY, pp. 147–159. https://doi.org/10.1007/978-1-4614-3445-0_14
Alquier, M., Kassim, C., Bertron, A., Sablayrolles, C., Rafrafi, Y., Albrecht, A., Erable, B., 2014. Halomonas desiderata as a bacterial model to predict the possible biological nitrate reduction in concrete cells of nuclear waste disposals. J. Environ. Manage. 132, 32–41. https://doi.org/10.1016/j.jenvman.2013.10.013
Amen, T.W.M., Eljamal, O., Khalil, A.M.E., Matsunaga, N., 2018. Evaluation of sulfate-containing sludge stabilization and the alleviation of methanogenesis inhibitation at mesophilic temperature. J. Water Process Eng. 25, 212–221. https://doi.org/10.1016/j.jwpe.2018.08.004
Bagaria, F., Riba, O., Albrecht, A., Robinet, J.-C., Madé, B., Román-Ross, G., 2021. Predicting degradation of organic molecules in cementitious media. Prog. Nucl. Energy 140, 103888. https://doi.org/10.1016/j.pnucene.2021.103888
Bary, B., 2008. Simplified coupled chemo-mechanical modeling of cement pastes behavior subjected to combined leaching and external sulfate attack. Int. J. Numer. Anal. Methods Geomech. 32, 1791–1816. https://doi.org/10.1002/nag.696
Bertron, A., 2014. Understanding interactions between cementitious materials and microorganisms: a key to sustainable and safe concrete structures in various contexts. Mater. Struct. 47, 1787–1806. https://doi.org/10.1617/s11527-014-0433-1
Bertron, A., Duchesne, J., 2013. Attack of Cementitious Materials by Organic Acids in Agricultural and Agrofood Effluents, in: Alexander, M., Bertron, A., De Belie, N. (Eds.), Performance of Cement-Based Materials in Aggressive Aqueous Environments. Springer Netherlands, Dordrecht, pp. 131–173. https://doi.org/10.1007/978-94-007-5413-3_6
Bertron, A., Duchesne, J., Escadeillas, G., 2007. Degradation of cement pastes by organic acids. Mater. Struct. 40, 341–354. https://doi.org/10.1617/s11527-006-9110-3
Bertron, A., Duchesne, J., Escadeillas, G., 2005a. Accelerated tests of hardened cement pastes alteration by organic acids: analysis of the pH effect. Cem. Concr. Res. 35, 155–166. https://doi.org/10.1016/j.cemconres.2004.09.009
Bertron, A., Duchesne, J., Escadeillas, G., 2005b. Attack of cement pastes exposed to organic acids in manure. Cem. Concr. Compos. 27, 898–909. https://doi.org/10.1016/j.cemconcomp.2005.06.003
Bertron, A., Escadeillas, G., de Parseval, P., Duchesne, J., 2009. Processing of electron microprobe data from the analysis of altered cementitious materials. Cem. Concr. Res. 39, 929–935. https://doi.org/10.1016/j.cemconres.2009.06.011
Bradley, A.S., Leavitt, W.D., Johnston, D.T., 2011. Revisiting the dissimilatory sulfate reduction pathway. Geobiology 9, 446–457. https://doi.org/10.1111/j.1472-4669.2011.00292.x
Chang, Y.C., Le Puil, M., Biggerstaff, J., Randall, A.A., Schulte, A., Taylor, J.S., 2003. Direct estimation of biofilm density on different pipe material coupons using a specific DNA-probe. Mol. Cell. Probes 17, 237–243. https://doi.org/10.1016/j.mcp.2003.07.004
Chen, Y., Ruhyadi, R., Huang, J., Yan, W., Wang, G., Shen, N., Hanggoro, W., 2021. Comprehensive comparison of acidic and alkaline anaerobic fermentations of waste activated sludge. Bioresour. Technol. 323, 124613. https://doi.org/10.1016/j.biortech.2020.124613
Dauzères, A., Le Bescop, P., Cau-Dit-Coumes, C., Brunet, F., Bourbon, X., Timonen, J., Voutilainen, M., Chomat, L., Sardini, P., 2014. On the physico-chemical evolution of low-pH and CEM I cement pastes interacting with Callovo-Oxfordian pore water under its in situ CO2 partial pressure. Cem. Concr. Res. 58, 76–88. https://doi.org/10.1016/j.cemconres.2014.01.010
Davis, J.A., 1984. Complexation of trace metals by adsorbed natural organic matter. Geochim. Cosmochim. Acta 48, 679–691. https://doi.org/10.1016/0016-7037(84)90095-4

907 Duchesne, J., Bertron, A., 2013. Leaching of Cementitious Materials by Pure Water and Strong Acids
908 (HCl and HNO3), in: Alexander, M., Bertron, A., De Belie, N. (Eds.), Performance of Cement-
909 Based Materials in Aggressive Aqueous Environments. Springer Netherlands, Dordrecht, pp.
910 91–112. https://doi.org/10.1007/978-94-007-5413-3_4
911 Duran, N., Seabra, A., 2012. Microbial Syntheses of Metallic Sulfide Nanoparticles: An Overview. Curr.
912 Biotechnol. E 1, 287–296. https://doi.org/10.2174/2211550111201040287
913 Durban, N., Rafrafi, Y., Rizoulis, A., Albrecht, A., Robinet, J.-C., Lloyd, J.R., Bertron, A., Erable, B., 2018.
914 Nitrate and nitrite reduction at high pH in a cementitious environment by a microbial
915 microcosm. Int. Biodeterior. Biodegrad. 134, 93–102.
916 https://doi.org/10.1016/j.ibiod.2018.08.009
917 Durban, N., Sonois-Mazars, V., Albina, P., Bertron, A., Albrecht, A., Robinet, J.-C., Erable, B., 2020.
918 Nitrate and nitrite reduction activity of activated sludge microcosm in a highly alkaline
919 environment with solid cementitious material. Int. Biodeterior. Biodegrad. 151, 104971.
920 https://doi.org/10.1016/j.ibiod.2020.104971
921 El Houari, A., Ranchou-Peyruse, M., Ranchou-Peyruse, A., Dakdaki, A., Guignard, M., Idouhammou, L.,
922 Bennisse, R., Bouterfass, R., Guyoneaud, R., Qatibi, A.-I., 2017. Desulfobulbus oligotrophicus
923 sp. nov., a sulfate-reducing and propionate-oxidizing bacterium isolated from a municipal
924 anaerobic sewage sludge digester. Int. J. Syst. Evol. Microbiol. 67, 275–281.
925 https://doi.org/10.1099/ijsem.0.001615
926 Ersan, Y.C., Boon, N., De Belie, N., 2018. Granules with activated compact denitrifying core (ACDC) for
927 self-healing concrete with corrosion protection functionality. Presented at the Final
928 conference of RILEM TC 253-MCI: Microorganisms-cementitious materials interactions,
929 RILEM Publications, pp. 475–484.
930 Etim, I.-I.N., Dong, J., Wei, J., Nan, C., Pokharel, D.B., Umoh, A.J., Xu, D., Su, M., Ke, W., 2021. Effect of
931 organic silicon quaternary ammonium salts on mitigating corrosion of reinforced steel
932 induced by SRB in mild alkaline simulated concrete pore solution. J. Mater. Sci. Technol., SI:
933 Advanced Corrosion-Resistant Materials and Emerging Applications 64, 126–140.
934 https://doi.org/10.1016/j.jmst.2019.10.006
935 Ewing, R.C., Whittleston, R.A., Yardley, B.W.D., 2016. Geological Disposal of Nuclear Waste: a Primer.
936 Elements 12, 233–237. https://doi.org/10.2113/gselements.12.4.233
937 Flemming, H.C., Wingender, J., 2010. The biofilm matrix. Nat. Rev. Microbiol. 8, 623–633.
938 https://doi.org/10.1038/nrmicro2415
939 Gallé, C., Peycelon, H., Le Bescop, P., Bejaoui, S., L'Hostis, V., Bary, B., Bouniol, P., Richet, C., 2006.
940 Concrete long-term behaviour in the context of nuclear waste management: Experimental
941 and modelling research strategy. J. Phys. IV Proc. 136, 25–38.
942 https://doi.org/10.1051/jp4:2006136004
943 Genthner, B.R.S., Devereux, R., 2015. Desulfomicrobium, in: Bergey's Manual of Systematics of
944 Archaea and Bacteria. American Cancer Society, pp. 1–9.
945 https://doi.org/10.1002/9781118960608.gbm01032
946 Giroudon, M., Peyre Lavigne, M., Patapy, C., Bertron, A., 2021. Blast-furnace slag cement and
947 metakaolin based geopolymer as construction materials for liquid anaerobic digestion
948 structures: Interactions and biodeterioration mechanisms. Sci. Total Environ. 750, 141518.
949 https://doi.org/10.1016/j.scitotenv.2020.141518
950 Goeres, D.M., Nielsen, P.H., Smidt, H.D., Frølund, B., 1998. The effect of alkaline pH conditions on a
951 sulphate reducing consortium from a Danish district heating plant. Biofouling 12, 273–286.
952 https://doi.org/10.1080/08927019809378360
953 Gutierrez, O., Park, D., Sharma, K.R., Yuan, Z., 2009. Effects of long-term pH elevation on the sulfate-
954 reducing and methanogenic activities of anaerobic sewer biofilms. Water Res. 43, 2549–
955 2557. https://doi.org/10.1016/j.watres.2009.03.008
956 Hai, T., Lange, D., Rabus, R., Steinbüchel, A., 2004. Polyhydroxyalkanoate (PHA) Accumulation in
957 Sulfate-Reducing Bacteria and Identification of a Class III PHA Synthase (PhaEC) in

Desulfococcus multivorans. Appl. Environ. Microbiol. 70, 4440–4448. https://doi.org/10.1128/AEM.70.8.4440-4448.2004
Hammes, F., Verstraete, W., 2002. Key roles of pH and calcium metabolism in microbial carbonate precipitation. Rev. Environ. Sci. Biotechnol. 1, 3–7. https://doi.org/10.1023/A:1015135629155
Iino, T., Mori, K., Uchino, Y., Nakagawa, T., Harayama, S., Suzuki, K.-I., 2010. Ignavibacterium album gen. nov., sp. nov., a moderately thermophilic anaerobic bacterium isolated from microbial mats at a terrestrial hot spring and proposal of Ignavibacteria classis nov., for a novel lineage at the periphery of green sulfur bacteria. Int. J. Syst. Evol. Microbiol. 60, 1376–1382. https://doi.org/10.1099/ijs.0.012484-0
Joshi, S., Goyal, S., Mukherjee, A., Reddy, M.S., 2017. Microbial healing of cracks in concrete: a review. J. Ind. Microbiol. Biotechnol. 44, 1511–1525. https://doi.org/10.1007/s10295-017-1978-0
Kuippers, G., Bassil, N.M., Boothman, C., Bryan, N., Lloyd, J.R., 2015. Microbial degradation of isosaccharinic acid under conditions representative for the far field of radioactive waste disposal facilities. Mineral. Mag. 79, 1443–1454. https://doi.org/10.1180/minmag.2015.079.6.19
Lagerblad, B., Traegaardh, J., 1994. Conceptual model for concrete long time degradation in a deep nuclear waste repository (Technical Report No. SKB-TR-95-21). Swedish Nuclear Fuel and Waste Management Co., Stockholm (Sweden).
Larreur-Cayol, S., Bertron, A., Escadeillas, G., 2011. Degradation of cement-based materials by various organic acids in agro-industrial waste-waters. Cem. Concr. Res. 41, 882–892. https://doi.org/10.1016/j.cemconres.2011.04.007
Liu, L., Ji, J., Guo, Y., Chen, J., 2021. Use of ecological concrete for nutrient removal in coastal sediment and its effects on sediment microbial communities. Mar. Pollut. Bull. 162, 111911. https://doi.org/10.1016/j.marpolbul.2020.111911
Liu, Y., Li, X., Kang, X., Yuan, Y., Du, M., 2014. Short chain fatty acids accumulation and microbial community succession during ultrasonic-pretreated sludge anaerobic fermentation process: Effect of alkaline adjustment. Int. Biodeterior. Biodegrad. 94, 128–133. https://doi.org/10.1016/j.ibiod.2014.07.004
Machel, H.G., 2001. Bacterial and thermochemical sulfate reduction in diagenetic settings — old and new insights. Sediment. Geol. 140, 143–175. https://doi.org/10.1016/S0037-0738(00)00176-7
Magniont, C., Coutand, M., Bertron, A., Cameleyre, X., Lafforgue, C., Beaufort, S., Escadeillas, G., 2011. A new test method to assess the bacterial deterioration of cementitious materials. Cem. Concr. Res. 41, 429–438. https://doi.org/10.1016/j.cemconres.2011.01.014
Menéndez, E., Matschei, T., Glasser, F.P., 2013. Sulfate Attack of Concrete, in: Alexander, M., Bertron, A., De Belie, N. (Eds.), Performance of Cement-Based Materials in Aggressive Aqueous Environments: State-of-the-Art Report, RILEM TC 211 - PAE, RILEM State-of-the-Art Reports. Springer Netherlands, Dordrecht, pp. 7–74. https://doi.org/10.1007/978-94-007-5413-3_2
Mu, T., Xing, J., Yang, M., 2019. Sulfate reduction by a haloalkaliphilic bench-scale sulfate-reducing bioreactor and its bacterial communities at different depths. Biochem. Eng. J. 147, 100–109. https://doi.org/10.1016/j.bej.2019.04.008
Muyzer, G., Stams, A.J.M., 2008. The ecology and biotechnology of sulphate-reducing bacteria. Nat. Rev. Microbiol. https://doi.org/10.1038/nrmicro1892
Pallud, C., Van Cappellen, P., 2006. Kinetics of microbial sulfate reduction in estuarine sediments. Geochim. Cosmochim. Acta 70, 1148–1162. https://doi.org/10.1016/j.gca.2005.11.002
Peckmann, J., Paul, J., Thiel, V., 1999. Bacterially mediated formation of diagenetic aragonite and native sulfur in Zechstein carbonates (Upper Permian, Central Germany). Sediment. Geol. 126, 205–222. https://doi.org/10.1016/S0037-0738(99)00041-X

Planel, D., Sercombe, J., Le Bescop, P., Adenot, F., Torrenti, J.-M., 2006. Long-term performance of cement paste during combined calcium leaching–sulfate attack: kinetics and size effect. Cem. Concr. Res. 36, 137–143. https://doi.org/10.1016/j.cemconres.2004.07.039

Qian, Z., Tianwei, H., Mackey, H.R., van Loosdrecht, M.C.M., Guanghao, C., 2019. Recent advances in dissimilatory sulfate reduction: From metabolic study to application. Water Res. 150, 162–181. https://doi.org/10.1016/j.watres.2018.11.018

Rafrafi, Y., Durban, N., Bertron, A., Albrecht, A., Robinet, J.-C., Erable, B., 2017. Use of a continuous-flow bioreactor to evaluate nitrate reduction rate of Halomonas desiderata in cementitious environment relevant to nuclear waste deep repository. Biochem. Eng. J. 125, 161–170. https://doi.org/10.1016/j.bej.2017.05.016

Rafrafi, Y., Ranaivomanana, H., Bertron, A., Albrecht, A., Erable, B., 2015. Surface and bacterial reduction of nitrate at alkaline pH: Conditions comparable to a nuclear waste repository. Int. Biodeterior. Biodegrad. 101, 12–22. https://doi.org/10.1016/j.ibiod.2015.03.013

Ragu Nandhakumar, S., Rajeshkumar, S., Anand, R.S., Malyla, V., Dua, K., Ezhilarasan, D., Lakshmi, T., 2022. Chapter 20 - Biogenic metal sulfide nanoparticles synthesis and applications for biomedical and environmental technology, in: Abd-Elsalam, K.A., Periakaruppan, R., Rajeshkumar, S. (Eds.), Agri-Waste and Microbes for Production of Sustainable Nanomaterials, Nanobiotechnology for Plant Protection. Elsevier, pp. 495–506. https://doi.org/10.1016/B978-0-12-823575-1.00027-5

Ravot, G., Garcia, J., Magot, M., Ollivier, B., 2015. Fusibacter. https://doi.org/10.1002/9781118960608.gbm00723

Rizoulis, A., Steele, H.M., Morris, K., Lloyd, J.R., 2012. The potential impact of anaerobic microbial metabolism during the geological disposal of intermediate-level waste. Mineral. Mag. 76, 3261–3270. https://doi.org/10.1180/minmag.2012.076.8.39

Rout, S.P., Charles, C.J., Garratt, E.J., Laws, A.P., Gunn, J., Humphreys, P.N., 2015. Evidence of the Generation of Isosaccharinic Acids and Their Subsequent Degradation by Local Microbial Consortia within Hyper-Alkaline Contaminated Soils, with Relevance to Intermediate Level Radioactive Waste Disposal. Plos One 10, e0119164. https://doi.org/10.1371/journal.pone.0119164

Sellier, A., Lacarrière, L., Gonnouni, M.E., Bourbon, X., 2011. Behavior of HPC nuclear waste disposal structures in leaching environment. Nucl. Eng. Des. - NUCL ENG DES 241, 402–414. https://doi.org/10.1016/j.nucengdes.2010.11.002

Sorokin, D.Y., Banciu, H.L., Muyzer, G., 2015. Functional microbiology of soda lakes. Curr. Opin. Microbiol. 25, 88–96. https://doi.org/10.1016/j.mib.2015.05.004

Sorokin, D.Y., Berben, T., Melton, E.D., Overmars, L., Vavourakis, C.D., Muyzer, G., 2014. Microbial diversity and biogeochemical cycling in soda lakes. Extremophiles 18, 791–809. https://doi.org/10.1007/s00792-014-0670-9

Sorokin, D.Y., Tourova, T.P., Panteleeva, A.N., Muyzer, G., 2012. Desulfonatronobacter acidivorans gen. nov., sp. nov. and Desulfobulbus alkaliphilus sp. nov., haloalkaliphilic heterotrophic sulfate-reducing bacteria from soda lakes. Int. J. Syst. Evol. Microbiol. 62, 2107–2113. https://doi.org/10.1099/ijs.0.029777-0

Sousa, J.A.B., Plugge, C.M., Stams, A.J.M., Bijmans, M.F.M., 2015. Sulfate reduction in a hydrogen fed bioreactor operated at haloalkaline conditions. Water Res. 68, 67–76. https://doi.org/10.1016/j.watres.2014.09.035

van Loon, L.R., Hummel, W., 1999. The Degradation of Strong Basic Anion Exchange Resins and Mixed-Bed Ion-Exchange Resins: Effect of Degradation Products on Radionuclide Speciation. Nucl. Technol. 128, 388–401. https://doi.org/10.13182/NT99-A3039

vanGinkel, C.G., Vandenbroucke, K.L., Stroo, C.A., 1997. Biological removal of EDTA in conventional activated-sludge plants operated under alkaline conditions. Bioresour. Technol. 59, 151–155. https://doi.org/10.1016/s0960-8524(96)00158-7

Vijay, K., Murmu, M., Deo, S.V., 2017. Bacteria based self healing concrete – A review. Constr. Build. Mater. 152, 1008–1014. https://doi.org/10.1016/j.conbuildmat.2017.07.040

Vinsot, A., Mettler, S., Wechner, S., 2008a. In situ characterization of the Callovo-Oxfordian pore water composition. Phys. Chem. Earth Parts ABC 33, S75–S86. https://doi.org/10.1016/j.pce.2008.10.048

Vinsot, A., Mettler, S., Wechner, S., 2008b. In situ characterization of the Callovo-Oxfordian pore water composition. Phys. Chem. Earth Parts ABC 33, S75–S86. https://doi.org/10.1016/j.pce.2008.10.048

Voegel, C., Bertron, A., Erable, B., 2016. Mechanisms of cementitious material deterioration in biogas digester. Sci. Total Environ. 571, 892–901. https://doi.org/10.1016/j.scitotenv.2016.07.072

Voegel, C., Bertron, A., Erable, B., 2015. Biodeterioration of cementitious materials in biogas digester. Matér. Tech. 103, 202. https://doi.org/10.1051/mattech/2015023

Voegel, C., Durban, N., Bertron, A., Landon, Y., Erable, B., 2019a. Evaluation of microbial proliferation on cementitious materials exposed to biogas systems. Environ. Technol. 1–11. https://doi.org/10.1080/09593330.2019.1567610

Voegel, C., Giroudon, M., Bertron, A., Patapy, C., Matthieu, P.L., Verdier, T., Erable, B., 2019b. Cementitious materials in biogas systems: Biodeterioration mechanisms and kinetics in CEM I and CAC based materials. Cem. Concr. Res. 124, 105815. https://doi.org/10.1016/j.cemconres.2019.105815

Widdel, F., Pfennig, N., 1981. Studies on dissimilatory sulfate-reducing bacteria that decompose fatty acids. I. Isolation of new sulfate-reducing bacteria enriched with acetate from saline environments. Description of Desulfobacter postgatei gen. nov., sp. nov. Arch. Microbiol. 129, 395–400. https://doi.org/10.1007/BF00406470

Zheng, Y., Xiao, Y., Yang, Z.-H., Wu, S., Xu, H.-J., Liang, F.-Y., Zhao, F., 2014. The bacterial communities of bioelectrochemical systems associated with the sulfate removal under different pHs. Process Biochem. 49, 1345–1351. https://doi.org/10.1016/j.procbio.2014.04.019